INVESTIGATION OF THE IMPACT OF SYNTHETIC INERTIA ON THE DYNAMICS OF POWER SYSTEMS

A Diploma Thesis submitted to attain the degree of

DIPLOM-INGENIEURS (Dipl.-Ing.) of TU WIEN

Supervised by

Univ.-Prof. Dr.-Ing. Wolfgang Gawlik

Submitted at

Vienna University of Technology

Faculty of Electrical Engineering and Information Technology

Institute for Energiesysteme und Elektrische Antriebe

Presented by

Alireza Kerdegarbakhsh

01226070

TU WIEN

Gusshausstr. 25/370,

A-1040 Wien,

Internet: http://www.ea.tuwien.ac.at

…To my fantastic wife

"It's too bad if a heart lacks fire,

and is deprived of the light

of a heart ablaze.

The day on which you are

without passionate love

is the most wasted day of your life."

– **OMAR KHAYYAM, The Rubáiyát of Omar Khayyám**

18 May 1048 – 4 December 1131

ACKNOWLEDGEMENTS

First and foremost, I would like to highly appreciate Prof. Wolfgang Gawlik for the generous support and professional supervision on this master thesis as well as providing me the chance to work on this theme at Institute of energy systems and electrical drives of TU Wien and giving me the precious opportunity to take part into the project “ABS4TSO” which yielded me many valuable insights on new control concepts for low inertia power system. Prof. Gawlik is a passionate scientist, an impressive leader and an outstanding academic head with consolidated excellent institutional and social skills. For me it is a great honor to do this work under supervision of Prof. Gawlik and it is even greater if this collaboration will be expanded further in the future.

Moreover, I thank Prof. Andreas Kugi and Prof. Georg Schitter at the automation and control institute of TU Wien who made me profoundly familiar with complex dynamical systems and enabled me to acquire deep comprehension of control systems.

Eventually, I would like to thank my fantastic wife, who was an abiding provenance of sacrifices, encouragement and patience. Without all her given supports, confidence and persuasion definitely I was not able to finish this extreme difficult way.

ABSTRACT

This thesis fundamentally deals with Small signal stability analysis of interconnected power systems influenced by decline in the total inertia of the grid.

Frequency stability is considered as a main part of this analysis which is done on non-linear multi-machine two area power system model.

In conventional power systems, big scale synchronous machines are referred to the major parts of the system which their moment of inertia play a vital role to keep power system stable against small disturbances.

While the growing share of renewable-based distributed generation, such as wind and solar power plants, on power systems lead to decrease in utilizing the conventional synchronous-based generation but it causes fading effectiveness of the task of moment of inertia on the grid as a figure in lowering system dynamic [1]. In other words, as it will be shown in the following chapters, lowering of moment of inertia is terminated a power system with lower robustness and higher sensitivity to small disturbances [1].

On the other hand, the inherent uncertainty that exists in renewable-based generations, due to their dependence on the weather conditions, results to increase of occurrence of disturbances remarkably and frequently. This undetermined behavior in turn threatens the stability of the system further and makes the system more unreliable [2].

Since the moment of inertia inherently makes slowing down the response of the system to disturbances then it causes to save more time for primary frequency controls to take action [3]. The lower moment of inertia in the system the faster frequency actions are essential [3]. As will be discussed, in integrated power systems keeping the frequency of the system still stable against the disturbances, like variation of the loads, by the slow conventional control actions like droop control and automatic voltage control seems to be inefficient.

Hence, the concept of synthetic inertia as a fast frequency response control technique is investigated how effective this solution can overcome the above mentioned rising challenges.

ZUSAMMENFASSUNG

Diese Arbeit befasst sich im Wesentlichen mit der Analyse der Kleinsignalstabilität von miteinander verbundenen Stromversorgungssystemen, die durch die Abnahme der Gesamtträgheit des Netzes beeinflusst werden.

Die Frequenzstabilität wird als Hauptbestandteil dieser Analyse betrachtet, die an einem nichtlinearen zwei verbundenen Stromversorgungssystemen mit mehreren Maschinen durchgeführt wird.

In konventionellen Stromversorgungssystemen werden große Synchronmaschinen auf die Hauptteile des Systems bezogen, deren Trägheitsmoment eine entscheidende Rolle spielt, um die Stabilität des Stromversorgungssystems gegen kleine Störungen zu gewährleisten.

Der wachsende Anteil erneuerbarer dezentraler Stromerzeugung wie Wind- und Solarkraftwerke auf Stromversorgungssystemen führt jedoch zu einer geringeren Nutzung der konventionellen synchronen Stromerzeugung, was dazu führt, dass die Wirksamkeit der Aufgabe des Trägheitsmoments im Netz nachlässt als Figur bei der Senkung der Systemdynamik. Mit anderen Worten, wie in den folgenden Kapiteln gezeigt wird, wird das Fehlen eines Trägheitsmoments durch ein Stromversorgungssystem mit geringerer Robustheit und Empfindlichkeit gegenüber kleinen Störungen beendet.

Andererseits führt die inhärente Unsicherheit, die bei Generationen auf erneuerbarer Basis aufgrund ihrer Abhängigkeit von den Wetterbedingungen besteht, dazu, dass das Auftreten von Störungen bemerkenswert und häufig zunimmt. Dieses unbestimmte Verhalten gefährdet wiederum die Stabilität des Systems weiter und macht das System unzuverlässiger.

Da das Trägheitsmoment die Reaktion des Systems auf Störungen von Natur aus verlangsamt, spart dies mehr Zeit, damit die Primärfrequenzsteuerungen Maßnahmen ergreifen können. Je geringer das Trägheitsmoment im System ist, desto schneller sind Frequenzaktionen erforderlich. Wie noch erläutert werden wird, scheint es in integrierten Stromversorgungssystemen ineffizient zu sein, die Frequenz des Systems gegenüber Störungen wie Schwankungen der Lasten durch langsame herkömmliche

Steueraktionen wie Statiksteuerung und automatische Spannungssteuerung stabil zu halten.

Daher wird das Konzept der synthetischen Trägheit als schnelle Frequenzgang steuerungstechnik untersucht, wie effektiv diese Lösung die oben erwähnte steigende Herausforderung bewältigen kann.

Contents

LIST OF FIGURES

LIST OF TABLES

1

1. INTRODUCTION

1.1 Preface

The need for energy, in its various forms, is an essential part of human life so that with the development of cities and movement toward progress and making more prosperity this need grows and become more critical. Based on 68th edition of BP statistical review of world energy published in year 2019, global energy demand over the year 2018 is going to continue to grow by 2.3%, nearly twice the average rate of growth since 2011 and its fastest rate this decade. Moreover, according to report, this remarkable growth of energy demand in recent decade is resulted by a robust global economy as well as higher heating and cooling needs in some parts of the world as indicated in FIG. 1 [4], [5], [6].

Besides to this above mentioned notable increase in global energy demand, still there exist a lot of areas all over the world, especially in developing countries, in which they have either no access to the modern forms of energy, like electricity, or their disposal to energy is very limited and somewhat unreliable compared to modern societies. For instance, in this among one and half billion human-being have no electricity and nearly three billion people cook over smoky wood, dung, or charcoal fires [7].

Now consider if we add these amount of people, who now have no or very finite access to modern form of energy, to the total global energy demand in future, we can easily estimate the huge amount of energy which be required in the coming years. Therefore, the type of energy that is exploited is doubly important in terms of available resources and, most importantly, its impact on the climate. Over the past two centuries, “fossil fuels” among the other forms of primary energy are still considered as a big part of the source of society’s energy [6], [8].

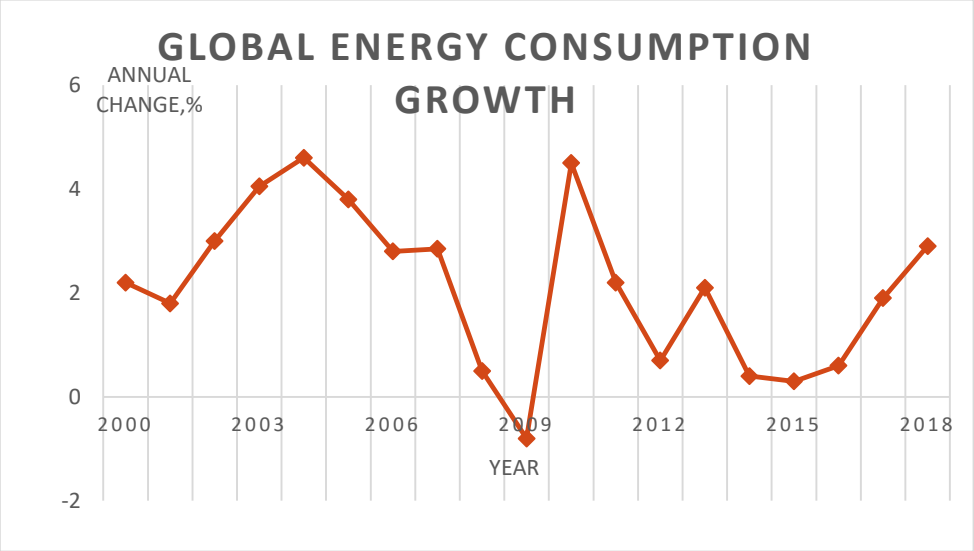

FIG. 1: This graph plots the actual annual change in primary energy consumption in the world over the almost two recent decades from year 2000 to 2018.

Data source: BP Statistical Review of World Energy 2019, 68th edition [5].

FIG. 2 indicates the share of each primary energy consumption in the world over the year 2018 based on BP Statistical Review of World Energy 2019, 68th edition [5]. According to this report and demonstration of figure 2, the largest shares of utilized world primary energy resources over the year 2018 came from only oil and natural gas accounting for nearly 45% of total energy demand while fossil fuels totally (Oil, natural Gas and Coal) show around 70% of world energy consumption. However, growth rate in renewables energy consumption is still located very far away to dominate the race as the first world primary energy source [6], [8].

Now the fossil fuels, from one side, are essential as the major source of energy to driven the progress and prosperity for human being, however on the other side, they are also considered as the main threats not only for human health but also for the global stability, for instance, through making pollution and climate change which can alone influences everything [7], [8]. It is notable to know that in addition to the carbon the other harms from burning fossil fuels such as sulfur dioxide, nitrogen dioxide, mercury, arsenic, acid gases, dioxins and other toxins are produced which all are damaging for environment as well as healthiness [8], [9]. For these reasons, we cannot keep our dependence on these harmful sources of energy and we need to find effective solutions to switch from fossil fuels to harmless energy sources [7], [8].

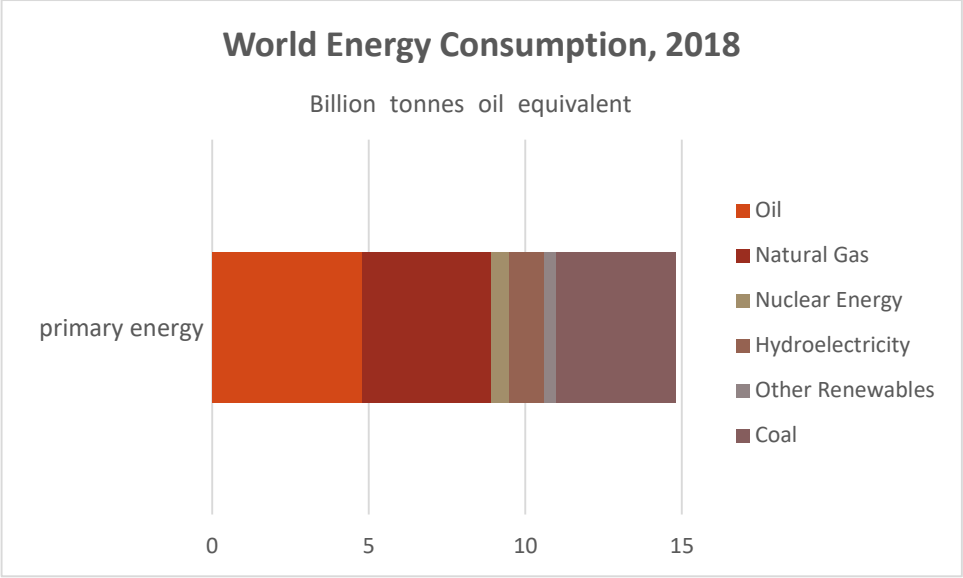

FIG. 2: The contribution of each primary source of energy in the world energy consumption over the year 2018. Data source: BP Statistical Review of World Energy 2019, 68th edition [5].

However, this major source of energy in the world (fossil fuel), directly or indirectly, is employed in all four main economic sections, i.e., building, transportation, industry and Electricity. In each part fossil fuel, as mentioned above, is still the leading source of energy despite all endeavors at replacing it with clean primary source of energy. As part of attempts toward this big evolution, one can mention increasing energy efficiency in the buildings and industry sectors or even electrify vehicles. In this among, Electricity generation alone is accounted for one the most significant consumer of fossil fuels and consequently contributes to around a forth of total greenhouse gas emissions. As indicated on FIG. 3, the global energy-related CO2 emissions increased by 1.7% to 33 Gigatonnes (Gt) in year 2018, while alone 10 Gt coal has been used for power generation [4], [10].

Electricity plays yet an effective role to power the other three main parts of energy consumption i.e., building, transportation and industry. As result, generating more clean electricity and bringing this clean electricity more into powering the other three sections can make a big progress toward preventing or even lowering greenhouse emissions. Renewable energy sources like solar and wind power plants can be considered as main green energy sources to generate clean electricity [3], [11], [12].

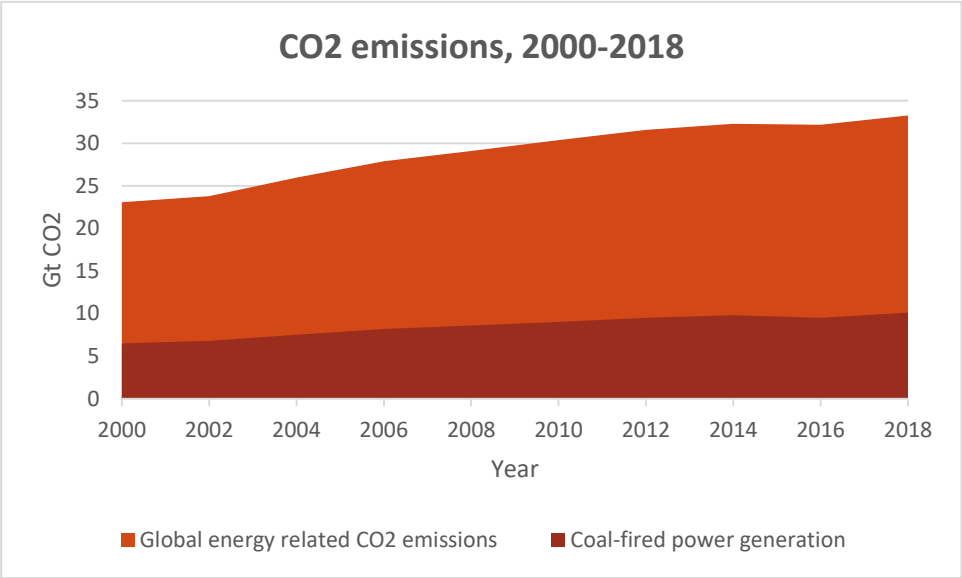

FIG. 3: This graph compares the share power generation sector in co2 emission in power generation sector with the other use of coal in recent two decades.

Data Source: International Energy Agency Reports, March 2019 & February 2020, [4], [10].

This is a strategy that most developed countries have already started to develop it to producing green energy. As for instance the U.S. electricity system planned to cover at least 80% of electricity needs through renewable energy resources by 2050 and global wind and solar installation is predicated to reach nearly 2200 gigawatts by 2030 compared to 1100 gigawatts in year 2018, an almost double growth!, [3], [11], [12].

1.2 Barriers for renewable energy

FIG. 4 shows the exponential rise of clean electricity generation from wind and solar energy sources. This exponential trend is from the world wind installation 17 gigawatts and solar installation 1.3 Gigawatts by year 2000, to over 500 Gigawatts for both wind and solar installation by year 2018. This is great in terms of preventing or even lowering CO2 emission [8], [11], [12].

However, for utilizing this clean energy we are faced with different challenges in various aspects from inherent fluctuation and uncertainty lying in this kind of energy to providing security and integration of them with conventional systems.

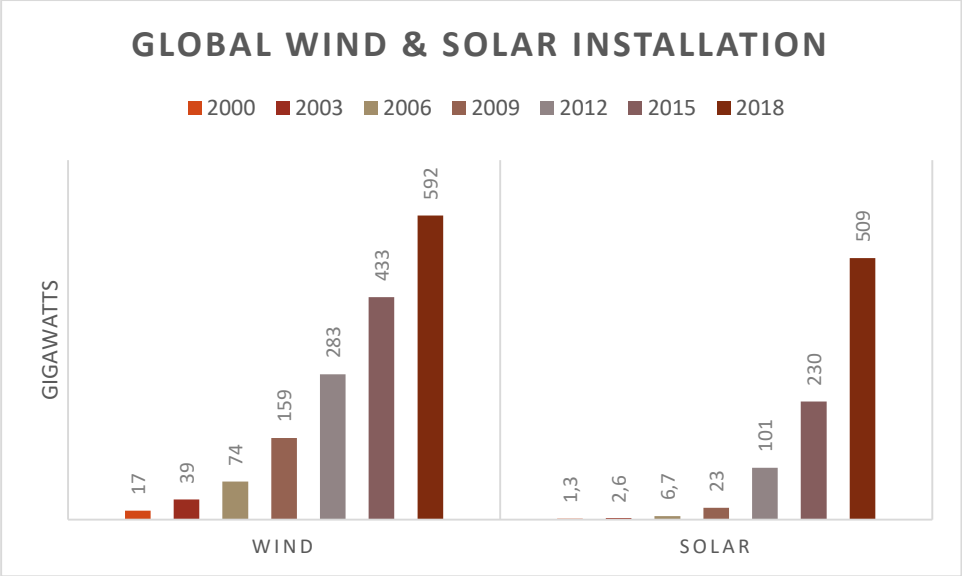

FIG. 4: Wind and solar power generation is expanding as the world shifts from fossil fuels to carbon free energy sources [5], [12].

1.3 Fluctuation of renewable energy sources

Large-scale penetration of renewable energy sources, in terms of wind and solar energy, leads to remarkable contribution of uncertain and fluctuating energy generation in the power system [3], [13]. They are entirely dependent to weather conditions, the time of the day and night, the season as well as geographical location so that their output fluctuates hourly all year round. For instance, solar power generation is normally higher in the summer and lower in the winter and wind is typically more in the spring and fall. Wind farms and solar panels cannot generate electricity when the wind doesn't blow or when the sun sets. In addition, they cannot be predicted with complete accuracy. These make the green energies really challenging because both solar power and wind power vary in both space and time (FIG. 5). As it will be discussed in the following chapters, this undetermined behavior challenges the stability and reliability of the power system [2], [13], [14].

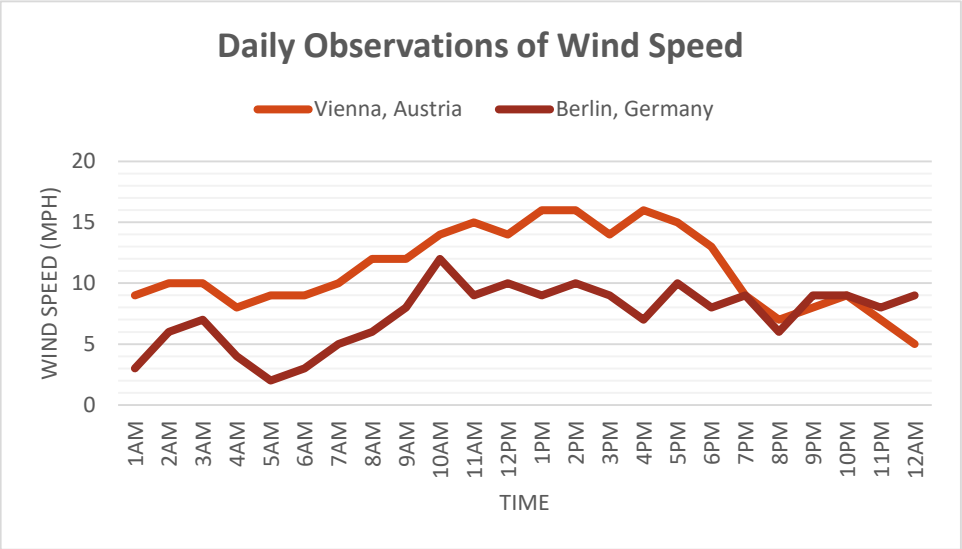

FIG. 5: This graph illustrates the variation of wind speed on 24 March 2020 for two different locations Vienna and Berlin [5], [14].

1.4 Digitalization, security and privacy

In order to make these variable energies more efficient and reliable, digital technologies are employed since they can provide a basis for data exchanges and analytics in a large scale and proper time as well as they can help the expansion of distributed energy resources which in turn making decisions technically more accurate and economically more optimum [15].

Digitalized energy systems can make balance between generation and consumption at the lowest cost. But employing Digitalization in energy sector, the same as other applications, are accompanied with security and privacy challenges. However, the remarkable difference is that the energy sector, as a critical infrastructure, is far more important so that it can make energy systems more vulnerable and appropriate target for cyber-attacks [15].

Moreover, as detailed data can assist the system performance and its flexibility, but data privacy can be considered as another major concern for consumers so that making balance between privacy and operational utilization of data should be taken into account in terms of adopting relevant policies [15].

1.5 Integration renewable sources with conventional power systems

In conventional power systems, big scale rotary synchronous machines are referred to the major parts of the system which their moment of inertia, provided by governor, plays a vital role to keep power system stable against small disturbances. This is because when small disturbances happen, the conventional primary control act with some delays in which the moment of inertia of big scale machines can effectively compensate this delay gap between the moment of occurrence of the disturbance and the response of primary control system. While integration of renewable energy sources in the power system is realized by power electronics technologies which will decrease the effectiveness of vital role of the moment of inertia in the power system in terms of frequency stability [3], [15], [16], [17].

In other word, as it will be discussed in the following chapters, lowering of the moment of inertia is terminated a power system with lower robustness and higher sensitivity to small disturbances [15], [16].

In addition to required proper control concepts to overcome the lack of effective amount of total inertia in the system, another possible future challenge to integrate big scale centralized (conventional) power plants with small scale distributed renewable energy sources will be the necessity of advanced communication systems owning a high level of cyber security and privacy property [8], [9], [15].

1.6 Summary and conclusions

We have now described the importance and necessity of using renewable energy sources to generating green energy and consequently to tackle threats of further climate change. But this scenario is accompanied with possible future challenges and risks for the world energy sector. This transformation of electricity will be complex and is faced with new waves of concerns from new faster control concepts to cyber security and privacy risks [8], [9]. Hence designing a system with efficient response time as well as with high flexibility and security grade in a cost- optimized integrated fashion by applying faster control and advanced communication systems seems to be essential.

Obviously, the design and decision we make in transformation of existed power system will affect our ability to handle probable risk later [8], [9].

1.7 Outline

The main approach in this thesis in order to investigate the impact of synthetic inertia on power system is based on [3] since we substitute synchronous machines with the constant power sources to simulate low inertia power system as well as using its phase-locked loop (PLL) concept to measure rate of change of frequency as input of our synthetic inertia model [3].

At chapter 2 we extract some formulation for single and multi-machine generally and especially for two area interconnected power grid based on linearized swing equation. Generally small signal stability analysis i.e. the small variations of frequency and rotor angle with respect to their nominal values is the main framework of this thesis. The investigation and formulation will be done in both time and frequency domains. The concept of synthetic inertia will be introduced as a control law proportional to the rate of change of frequency. The delay of measurement and system response is considered into the modeling of synthetic inertia as well. As the main duty of synthetic inertia would be for faster primary control action to provide frequency stability against small disturbances, hence we utilize a linear model of synthetic inertia however, at chapter 3, its effectiveness in a nonlinear power system model will be evaluated.

Chapter 3 is divided into 3 main parts including power system without any controller, equipped with just conventional controllers and with employing synthetic inertia additionally based on kundur's artificial model of two area power system (1993). We change the total inertia at each section to evaluate the influence of moment of inertia on different parameters of the system such as frequency of the grid, tie-line voltages and power flow through the tie-line. Finally, we observe placement of the synthetic inertia on dynamic behavior of low-inertia power system while as small disturbance simulation we increase the load of area 1, which sends energy to area 2, and simultaneously decreasing the total inertia at area 2.

2

2. POWER SYSTEM DYNAMICS

In this chapter we discuss the consequences of employing renewable energy sources on lowering critical parameter for system stability in integrated power system, called inertia constant. We discuss the effect of low inertia constant on a linear model for single and interconnected power system. In case of interconnected power system we consider an equivalent inertia constant for each assumed coherent area. A swing equation based synthetic inertia control concept will be introduced and its effect on system dynamics will be investigated accordingly. We analyze the dynamics of interconnected power system based on a derived transfer function for a two area power system in frequency and time domains as well [3].

2.1 Small Signal Stability; Disturbances; System Metrics

The stability of rotor angle of power system can be threatened by small or large disturbances. The system have to operate reliably against these disturbances and successfully supply the maximum amount of the load [18]. Conventional small disturbances take place continually in the form of small variations in loads and generations which considered in small signal stability analysis despite of large disturbances occurred in form of different kind of short circuits which in turn categorized as transient stability investigations. The small disturbances cause small excursions in rotor angle from its equilibrium point which allows us to linearize the equations of the system around the operating points [18].

The conventional small disturbances, however in normal situation, are predictable and follow load profile. By penetration of renewable energy sources we are faced with the

new nature of small disturbances events in integrated power grids as they decrease the order of predictability characteristic since they are inherently dependent on the environmental conditions. This uncertain characteristic and obviously more frequent occurrence of load-generation variations make some difficulty for traditional system operation to plan balancing between demand and supply and providing reliable system. Clearly the more frequent load-generation changes, the more flexible system with lower response time is required [3].

The situation will be more critical and more threatening for reliability and stability of the system in the same proportion as the amount of energy sources with uncontrollable characteristic are increased to connect to the grid. In addition to this frequent almost imprecise predictable characteristic of renewable energy sources, these power electronics based renewable energy sources have a remarkable effect to decrease the total inertia constant of the system since they do not provide any at all or low degree of inertia constant in power system. This lowering inertia constant in turn, as it will be discussed in the next sections, has notable implications on frequency dynamics of power system [2], [3].

The conventional power system are generally based on rotational synchronous machines which provide a fundamental property for system stability margin opposed to the small faults. Hence, a direct consequence of retiring synchronous generators in integrated power systems is the less contribution of these large scale machines and consequently utilizing the benefit of the moment of inertia of their rotors [13], [19].

While a small fault happens the primary control system needs around some ten seconds to recover resulted frequency deviation in which the moment of inertia can lower the rate of frequency deviation out of its nominal range [19]. It will be presented that the amount of total inertia in the power grid has direct effect on some system parameters like frequency nadir as well as the rate of change of frequency (RoCoF) immediately after happening small disturbance [3], [13], [18].

In low inertia power systems equipped with just traditional primary controls, the frequency deviates faster from its rated values and reaches lower frequency peak since the prime movers of the conventional power plants cannot response as fast as the rate of frequency changes [13].

This, in turn, will enhance the probability of further disconnections and protection tripping which ultimately would lead to blackout of entire system [13].

Hence, in order to restore the active power balance in proper time interval to maintain the grid frequency within its rated bounds and consequently preventing further faults and blackout as well, the faster primary control strategies seem to be essential to cover the infirmity of conventional primary controls facing with high rate frequency changes which normally can be realized by devices based on power electronics components [13].

2.2 Conventional Power Systems, Synchronous Machines and Inertia Constant

Power systems conventionally utilize primary sources of energy, including coal, oil and natural gas, nuclear and hydraulic to generate electricity. This conversion process typically is done through a prime mover (turbine) coupled with a synchronous generator which converts the mechanical energy to alternative current (AC) electrical energy. The AC electrical energy in turn is transported through transmission system where it should be consumed. All the time, the system have to continually maintain the frequency and voltage at a predefined set points as well as must possess a level of reliability to return the variables to nominal values at the right time in case of fault events. To meet this specification, several control systems at various location, from the prime mover to transmission system, with different time setting are engaged [13], [20].

This conventional synchronous machine based system must rotate permanently with constant angular velocity in order to keep the frequency of the system stable. To achieve this requirement, based on the mechanics of motion, all acting forces (torques) on machine must be balanced. In other word, any unbalanced force (torque) acting upon synchronous machine directly leads to angular acceleration and changing of the system frequency consequently. But, still based on this law of motion, the angular acceleration of the rotor of machine depends inversely on the mass (moment of inertia) of the rotor. This inverse relationship between angular acceleration and moment of inertia is determinative since the higher moment of inertia results in the lower angular acceleration (and slower frequency deviation) and vice versa [13], [20].

To formulation the above expressions, typically the swing equation is introduced in most associated technical literatures to describe synchronous machine dynamic behavior around the steady-state of operation. The acting forces upon on each machine are divided to driving mechanical torque and electromagnetic torque. The swing equation is represented in per unit as [13], [20]:

$$T_{acc,pu} = T_{mech,pu} - T_{elec,pu} = 2H\dot{\omega}_{pu} \tag{1.2}$$

where ω is per unit angular velocity, H inertia constant and T_{mech} and T_{elec} are the per unit mechanical torque and electrical torque respectively.

The inertia constant is defined as stored energy at nominal speed over apparent power as follow [3], [20]:

$$H = \frac{I\omega_{0,mech}{}^2}{2\,S_{base}} \tag{2.2}$$

$\omega_{0,mech}$ is nominal angular velocity in rad/sec, S_{base} the rated power of the machine and I the moment of inertia. However, the inertia constant of each machine is also considered as required time (in seconds) for rated torque to accelerate the rotor of generator from zero to rated speed which is expressed by (2H) [3], [20], [21].

The angular velocity of the rotor is related to the grid frequency f (or electrical angular velocity ω_{elec}) with the number of pole pair of synchronous machine p, hence

$$\omega_{mech} = \frac{2\pi f}{p} = \frac{\omega_{elec}}{p} \tag{3.2}$$

In which the per unit angular velocity is resulted from

$$\frac{\omega_{mech}}{\omega_{0,mech}} = \frac{\omega_{elec}/p}{\omega_{0,mech}/p} = \frac{\omega_{\mathrm{elec}}}{\omega_0} = \omega_{pu} \tag{4.2}$$

As the response of the system with respect to small deviation from nominal values is considered in which the steady state of the system is threatened after occurrence of a disturbance [22], then we can modify the per unit swing equation (1.2) as [13], [20], [22]:

$$\Delta P_{mech,pu} - \Delta P_{elec,pu} = 2H\Delta\dot{\omega}_{pu} \tag{5.2}$$

since

$$\omega_{pu} = \omega_{0,pu} + \Delta\omega_{pu}$$
$$\Delta P_{mech} - \Delta P_{elec} = \Delta T_{mech} - \Delta T_{elec} \quad (6.2)$$

Where (Δ) indicates the deviation of each parameter from its steady state value.

ΔP_{mech} and ΔP_{elec} are mechanical and electrical power changes from the steady state values that are conventionally resulted by speed governing system and variation of the load respectively.

If we consider the response of the loads to frequency deviations, therefore the (5.2) is expressed as:

$$\Delta P_{mech,pu} - \Delta P_{elec,pu} - \mathrm{D}\Delta\omega = 2H\dot{\Delta\omega}_{pu} \quad (7.2)$$

in which D is defined as load damping constant.

Respectively, we have the changes of load angle parameter $\Delta\delta$ around its rated values δ_0 as follows:

$$\Delta\delta = \omega t - \omega_0 t \quad (8.2)$$

that its first derivative over the time yields:

$$\dot{\Delta\delta} = \omega - \omega_0 \quad (9.2)$$

and by second derivative we reach:

$$\ddot{\Delta\delta} = \omega_0 \dot{\Delta\omega}_{pu} \quad (10.2)$$

which in turn by substituting (7.2) into (10.2) and considering synchronizing coefficient K, we have:

$$\frac{2H}{\omega_0}\ddot{\Delta\delta} + \frac{D}{\omega_0}\dot{\Delta\delta} + K\Delta\delta = \Delta P_{mech,pu} \quad (11.2)$$

Now we have a first and a second order differential equation with respect to angular velocity, (7.2), and angular position, (11.2), respectively that their transfer functions are derived in the next steps.

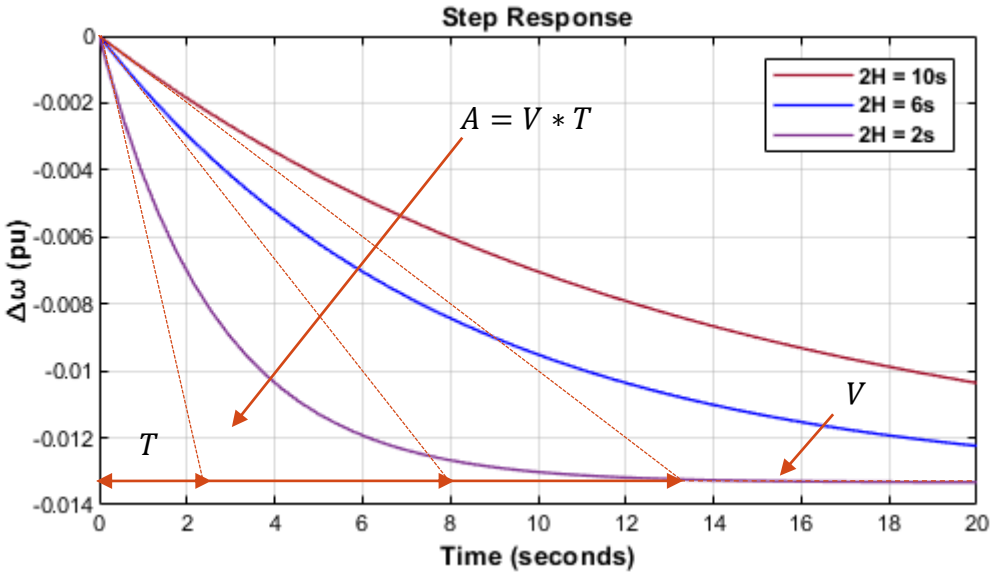

FIG. 6: Step response of frequency, for $D = 0.75$ and a step rise in load by $\Delta P_e = 0.01$ pu.

The transfer function of (7.2), by assuming no change happens in mechanical power, is resulted to [18], [23], [24]:

$$G_1(s) = \frac{\Delta\omega}{\Delta P_{acc}} = \frac{-V}{1 + sT} \tag{12.2}$$

with the gain factor $V = \Delta P_{elec}/D$ and time constant $T = 2H/D$ while D and H are load damping and inertia constants respectively.

The step response of (11.2) is derived as [24], [25]:

$$h(t) = \Delta\omega(t) = -V\left(1 - e^{-\frac{t}{T}}\right)\sigma(t) \tag{13.2}$$

and the associated impulse response is [24], [25]:

$$g(t) = \frac{d}{dt}\Delta\omega = \frac{V}{T}e^{-\frac{t}{T}}\sigma(t) \tag{14.2}$$

Equations (13.2) and (14.2) illustrate that frequency deviation of the system and the rate of its change (RoCoF) vary exponentially over the time and both of them are effected by the load damping and the inertia constant as well.

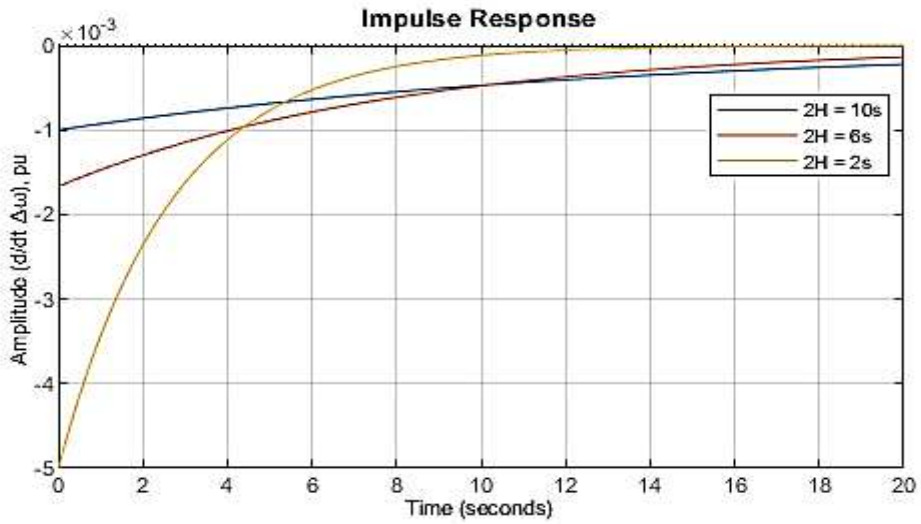

FIG. 7: Impulse response of frequency, for $D = 0.75$ and a step rise in load by $\Delta P_e = 0.01$ pu.

The inertia constant influences directly the time constant of exponential function, hence the reducing of the inertia constant leads to lower time constant which in turn results to faster frequency change [26]. For example, for $D = 0.75$ and a step rise in load by $\Delta P_{elec} = 0.01$ pu, the response of pu frequency as a function of time and for different values of inertia constant is shown in FIG. 6.

As illustrated, by reducing of the inertia constant the parameter T as well as the area $A = VT$ are decreased as we assume $V = Const$.

Moreover, the impulse response $\Delta\omega(t)$ is shown in FIG. 7 which indicates the rate of variation of frequency. This shows an inverse relation with inertia constant so that by lower values of inertia constant we observe faster frequency deviations from its nominal value [27].

For a system with infinite bus model the second order transfer function of equation (11.2) is derived as [20], [24], [25]:

$$\frac{\Delta\delta}{\Delta P_{acc}}(s) = G_2(s) = \frac{-V}{1 + 2\xi sT + (sT)^2}$$

$$V = \Delta P_{elec}/K \tag{15.2}$$

$$T = \sqrt{\frac{2H}{K\omega_0}} = \frac{1}{\omega_n}\ ;\ \xi = \frac{D}{2\sqrt{2HK\omega_0}}\ ;\ \omega_d = \omega_n\sqrt{1-\xi^2}$$

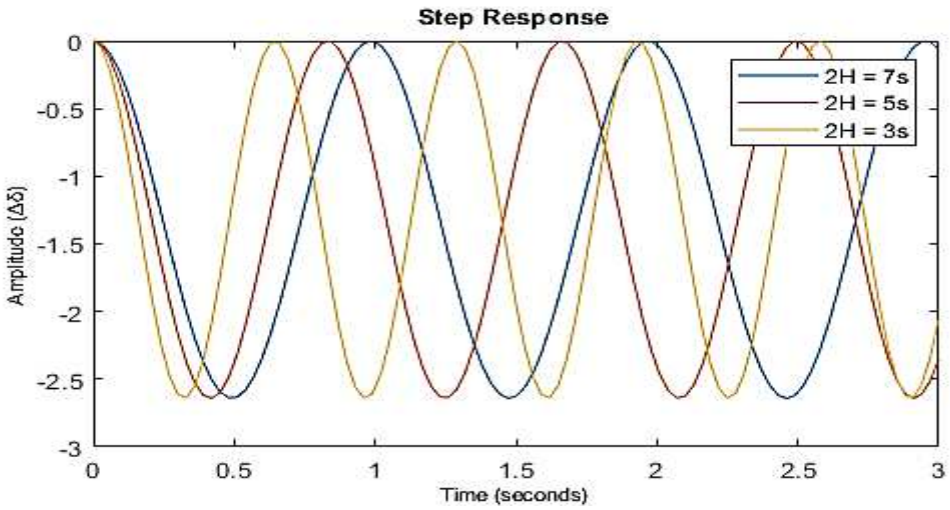

FIG. 8: the change of undamped natural frequency with respect to inertia constant.

where V is gain factor , $T > 0$ time constant , $0 \leq \xi < 1$ damping ratio , ω_n undamped natural frequency and ω_d damped frequency.

The step and impulse responses of (15.2) in a general form result in (16.2.1) and (16.2.2) respectively [24], [25]:

$$h(t) = -V\left(1 - \frac{1}{\sqrt{1-\xi^2}}\left(\xi \sin\left(\sqrt{1-\xi^2}\,\frac{t}{T}\right) + \sqrt{1-\xi^2}\cos\left(\sqrt{1-\xi^2}\,\frac{t}{T}\right)\right)e^{-\xi\frac{t}{T}}\right)\sigma(t) \qquad (16.2.1)$$

$$g(t) = \frac{-V}{T\sqrt{1-\xi^2}}e^{-\xi\frac{t}{T}}\sin\left(\sqrt{1-\xi^2}\,\frac{t}{T}\right)\sigma(t) \qquad (16.2.2)$$

For instance, the parameters such as damped frequency of oscillation, damping ratio and undamped natural frequency are determined for each of following values of inertia constant:

i) $2\mathrm{H} = 7\mathrm{s}$ ii) $2\mathrm{H} = 5\mathrm{s}$ iii) $2\mathrm{H} = 3\mathrm{s}$

with $D = 10.0$ and $K = 0.757$ (pu torque/rad) [20].

The following table shows the results for different values of inertia constant:

$2H$ (Sec.)	ξ	ω_n (Hz)	ω_d (Hz)
7	0.1120	1.0162	1.0098
5	0.1324	1.2024	1.1918
3	0.1709	1.5523	1.5295

Table 1: the effect of inertia constants on parameters such as damped frequency of oscillation, damping ratio and undamped natural frequency.

As Table 1 indicates, by decreasing of inertia constant we observe increase on damping factor as well as both undamped natural frequency and damped frequency, however the rise in frequency of oscillation is in the level of a few tenth while in the damping ratio as much as a few hundredth.

In addition, FIG. 8 illustrates the change of undamped natural frequency with respect to inertia constant as lower inertia causes higher frequency of oscillation based on the below formulation:

$$\frac{\omega_{n,1}}{\omega_{n,2}} = \sqrt{\frac{H_2}{H_1}}$$

All above formulations are for individual generator while in cases of multi machines and interconnected power system it is required to modify so far formulations.

2.3 Interconnected Power System and Equivalent Inertia

In power system a group of machines in each area work together to provide the required energy for its area. In order to increase the reliability of the grids the interconnection concept are issued to connect a group of machines located at a geographical synchronous area to another group at another area. This interconnection makes the system very more complex and furthermore analyze of the performance of each group of machines against the other groups should be taken into account. To do that, in case of coherent coupled machines in each area we can neglect the intermachine performances and consider the dynamic models of single machine for each group of coherent connected however with applying equivalent parameters [13], [20].

For instance, the inertia constant of this equivalent model is calculated based on (17.2). By the same manner an equivalent load-damping constant is calculated which indicates the effects of the system loads on the frequency dynamics.

As result, the equation of motion in case of interconnected power system can be formulated in the same manner like single machine but with equivalent parameters. For a system with n generators the equivalent parameters are given as [13], [20]:

$$H_{eq} = \frac{\sum_{i=1}^{n} H_i S_{base,i}}{\sum_{i=1}^{n} S_{base,i}} \qquad (17.2)$$

$S_{base,eq}$ is the system base, which is often obtained from the summation of all (synchronous) generation connected to the system.

2.4 Future Power System with Low System Inertia:

In the last section we saw the influence of inertia constant on the dynamic of frequency and angular displacement. Depending on the type of generation and contribution of each type, the total inertia constant in each synchronous area is quantified which can be used as a characteristic to analyze the power system operation and stability regarding small and large disturbances like load changes and short circuits.

Table 2 shows some typical values of parameter inertia constant for various types of power generation [28], [29].

These values of inertia constant differ from a range between 0-9 seconds which indicates invariant equivalent inertia for each time interval depending on the contribution of generation units for every synchronous area.

However, it is generally obvious that by more penetration of the generations like biomass, wind and solar, the equivalent inertia constant get smaller over time as these types of power supply present either no inertia at all or they have an inertia constant even less than half of conventional power supplies such as nuclear or thermal units.

Type of Power Generation			Inertia Constant, 2H (Sec)
Thermal Unit		3600 r/min	2.5 - 6.0
		1800 r/min	4.0 - 6
Turbine Generator	Condensing	1800 r/min	9.0 – 6.0
		3000 r/min	7.0 – 4.0
	Non-Condensing	3000 r/min	4.0 – 3.0
Water wheel	Slow (< 200 r/min)		2.0 – 3.0
	High (> 200 r/min)		2.0 – 4.0
Nuclear			7.0
Biomass			2.0
Other Renewable			2.0
Solar, Wind, Marine			0

Table 2: Typical inertia constant for some various kinds of power generation [28], [29].

Moreover, the report of ENTSO-E[1] dated 29 March 2017 declares the future energy scenario for 2030 Vision 4 (the highest occurring percent of Renewable Energy Sources, RES, in any hour of the year) so that eight countries in Europe reach an RLPI[2] of 100% on national basis and 22 countries at least 50% for the most challenging hours [30].

(FIG. 9) and (FIG. 10) illustrate the minimum and maximum inertia constant contribution arranged for four synchronous areas associated with the future energy scenario of 2030 Vision 4 at 50% and 90% duration points respectively [30].

For instance, Great Britain (GB) will represents an inertia constant of 2.1s at the program of 50 percent renewable energy source penetration and 0.7s for the 90 percent penetration.

Likewise in other synchronous areas, some countries will be showing very low inertia contribution in which Germany in CE synchronous area takes part only 0.6 s inertia constant at 50 percent duration point [31].

[1] European Network of Transmission System Operators for Electricity, 29 March 2017 [30].
[2] RES Load Penetration Index is defined as the maximum hourly variable RES coverage of load, e.g. for a country [30].

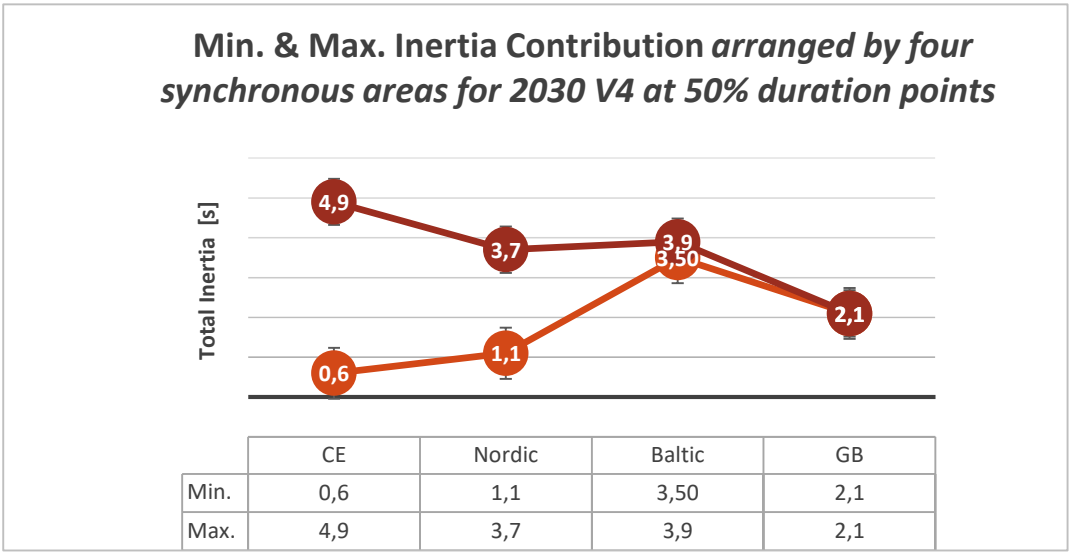

	CE	Nordic	Baltic	GB
Min.	0,6	1,1	3,50	2,1
Max.	4,9	3,7	3,9	2,1

FIG. 9: This figure illustrates Min. & Max Inertia Contribution for each Synchronous Area at 50% duration points arranged by synchronous areas for 2030 V4 (Source: ENTSO-E 29 March 2017) [31].

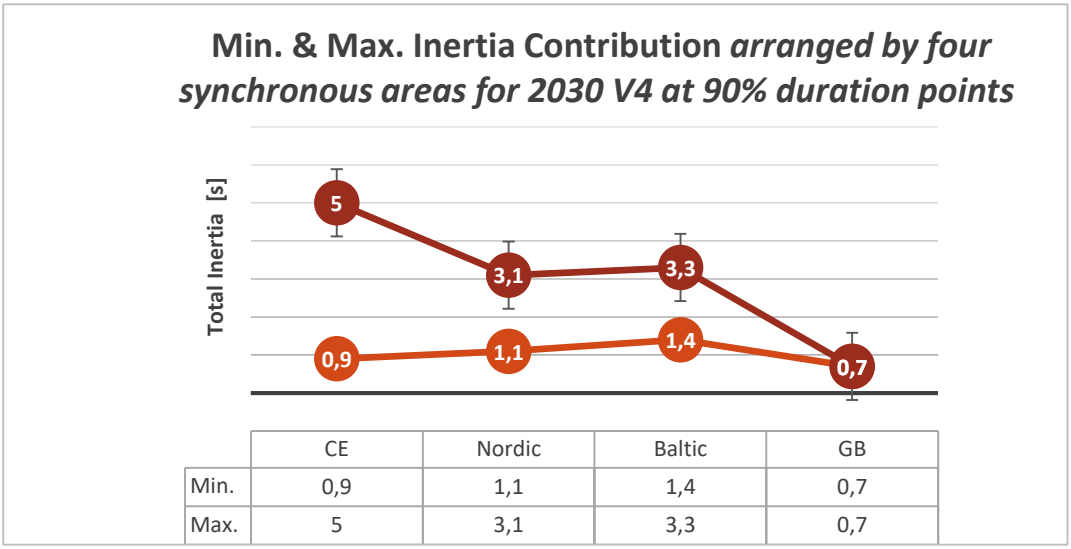

	CE	Nordic	Baltic	GB
Min.	0,9	1,1	1,4	0,7
Max.	5	3,1	3,3	0,7

FIG. 10: This figure illustrates Min. & Max Inertia Contribution for each Synchronous Area at 90% duration points arranged by synchronous areas for 2030 V4 (Source: ENTSO-E 29 March 2017) [31].

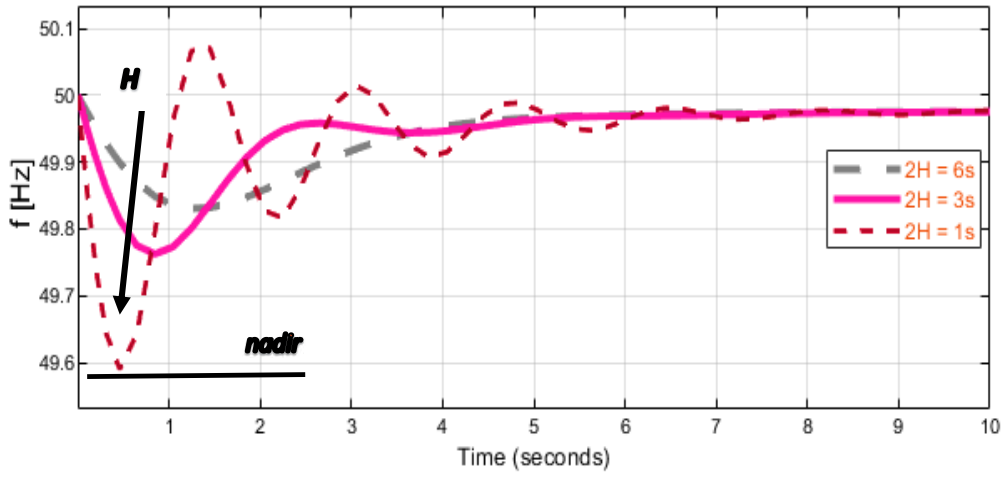

FIG. 11: The response a reheat steam turbine system for different values of inertia constant when faced with a step load change [20].

As result, these examples demonstrate a remarkable drop on inertia constant at various synchronous areas in the near future which in turn will be facing us with stability and reliability challenges, as discussed in the last section and also shown on FIG. 11.

FIG. 11 shows the response of a conventional generating unit with a reheat steam turbine when faced with a step load change. This response have been derived by using linearized model and parameter values from [20].

However other parameters like the type of boiler and its control or mode of operation can influence the system response and make it slower to some extent, the simulation results illustrate the notable different transient responses with respect to different inertia constants although the steady state frequency deviation stays the same for all three values of inertia. The differences in transient responses are remarkable in the rate of frequency drop as well as nadir values, shown on FIG. 11.

Besides, by decreasing Inertia value to 1s, the response of the system to a step increase in load demand demonstrates a damped oscillatory behavior which further shows the lack of efficiency of primary control to overcome demand changes in right time at low inertia power systems.

2.5 Multi-Machine Interconnected Power System

A non-linear interconnected alternative current (AC) power system consists of synchronous machines, buses and branches with various control actions such as governors, automatic voltage regulators (AVR), power system stabilizers (PSS) which employs to maintain the main parameters of the system including Voltage, frequency and rotor angle in the range of rated values. Generally, Differential-algebraic equations describe the dynamical model of the multi machine interconnected power system in which differential equations comprise both mechanical and electrical states of generation units and algebraic equations are derived from power or current balanced form of transmission network [3], [20], [29].

Now, we consider a graph model for power network with n nodes (buses) and maximum n x n transmission lines. By assuming of all buses as generation bus and neglecting the resistance of branches (Kron-reduction model) [20], the dynamics of the i^{th} generator (based on second order notation of swing equation) is formulated as [3], [22], [32]:

$$\frac{2H_i}{\omega_0}\frac{d^2(\Delta\delta_i)}{d^2t} + \frac{D_i}{\omega_0}\frac{d(\Delta\delta_i)}{dt} = \Delta P_{in\,pu,i} - \Delta P_{out\,pu,i} \qquad i \in \{1,\dots,n\} \tag{18.2}$$

where $P_{in\,pu,i}$and $P_{out\,pu,i}$ refer to the per unit mechanical power input and electrical power output respectively [3], [32].

$P_{out,i}$ is the total real electrical power which is consumed at bus i through the load directly connected to this bus plus real power injected to the network [33]:

$$\begin{aligned} P_{out,i} = P_{L,i} + P_{Network,i} &= P_{L,i} + Re\left(\bar{V}_i\left(\sum_{j=1}^{n} jb_{ij}\bar{V}_j\right)^*\right) \\ &= P_{L,i} + \sum_{j=1}^{n} V_i V_j b_{ij}\sin(\delta_i - \delta_j) \quad i = 1,\dots,n \end{aligned} \tag{19.2}$$

where V_i is the bus voltage amplitude and δ_i phase angle at bus i and b_{ij} is the susceptance related to line (branch) between buses (nodes) i and j. In case of Kron-reduction model in which all buses are modeled as generator and the set of passive load and line resistance are eliminated that leads to an equivalent transfer network that generation nodes are directly connected with each other [20], [33].

In terms of dynamics studies of rotor angle after occurrence of small disturbances we can assume constant voltage amplitude at each bus equals to one per unit as well as very small changes of phase angles between two buses, $|\Delta(\delta_i - \delta_j)| \ll 1$, in which we can express a linear form of $P_{out.i}$ as [3], [33]:

$$\Delta P_{out.i} = \Delta P_{L,i} + \sum_{j=1}^{n} b_{ij}\ \Delta(\delta_i - \delta_j) \quad i \in \{1, \ldots, n\} \tag{20.2}$$

In addition by considering Kron-reduction model we can simplify (18.2) as:

$$\frac{2H_i}{\omega_0}\frac{d^2(\Delta\delta_i)}{d^2t} + \frac{D_i}{\omega_0}\frac{d(\Delta\delta_i)}{dt} = -\Delta P_{L,i} - \sum_{j=1}^{n} b_{ij}\ \Delta(\delta_i - \delta_j) \quad i \in \{1, \ldots, n\} \tag{21.2}$$

where in case of constant mechanical power input we can eliminate $P_{in,i}$ as well [33].

To simplify the expression of (21.2) we substitute some notations as follows:

$$J_i = \frac{2H_i}{\omega_0};\ C_i = \frac{D_i}{\omega_0};\ \delta_i = \Delta\delta_i;\ \dot{\delta}_i = \frac{d(\Delta\delta_i)}{dt};\ \ddot{\delta}_i = \frac{d^2(\Delta\delta_i)}{d^2t};\ D_i = -\Delta P_{L,i}$$

As result we have [3], [22], [33]:

$$J_i\,\ddot{\delta}_i + C_i\,\dot{\delta}_i = D_i - \sum_{j=1}^{n} b_{ij}\ (\delta_i - \delta_j) \qquad i \in \{1, \ldots, n\} \tag{22.2}$$

The above formulation can also be used for interconnected power systems which every parameter should be substituted by equivalent values of each area and electrical power output is considered as real power injected to the tie lines.

However basically the equivalent swing equation is applicable in strongly coherent grid in each area, in which all related machines can be considered connected to the purposed bus as the center of inertia [3], [13], [32].

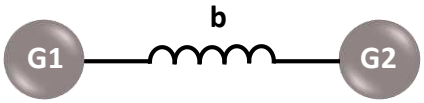

FIG. 12: Two area power system interconnected by susceptance b [33], [34].

2.6 Dynamics of a Two Areas Power System in Frequency Domain

In this section we will discuss the dynamics of two areas interconnected power system as a combination of two generators connected with transmission line with impedance coefficient b_{12} (FIG. 12). At first step, the dynamics of the system is considered by neglecting damping and synchronizing coefficients that from (22.2) we drive [3], [19], [35]:

$$\begin{aligned} J_1\ddot{\delta}_1 &= d - b_{12}(\delta_1 - \delta_2) \\ J_2\ddot{\delta}_2 &= -b_{21}(\delta_2 - \delta_1) = b_{12}(\delta_1 - \delta_2) \end{aligned} \tag{23.2}$$

As we assume the changing local load as disturbance ($d_i = -\Delta P_{L,i}$) just happens in area 1 then we have $d = \Delta P_{L,1}$ and $d_2 = 0$.

Laplace transform from (23.2) express the differential equations in the frequency domain:

$$\begin{aligned} J_1 s^2 \delta_1(s) &= d - b_{12}(\delta_1 - \delta_2) \\ J_2 s^2 \delta_2(s) &= b_{12}(\delta_1 - \delta_2) \end{aligned} \tag{24.2}$$

Respectively the transfer functions from $\delta_1(s)$ and $\delta_2(s)$ as outputs versus d as input are derived ($b_{12} = b$):

$$\begin{aligned} G_1(s) &= \frac{\delta_1}{d}(s) = \frac{J_2 s^2 + b}{J_1 J_2 s^4 + b(J_1 + J_2)s^2} \\ G_2(s) &= \frac{\delta_2}{d}(s) = \frac{b}{J_1 J_2 s^4 + b(J_1 + J_2)s^2} \end{aligned} \tag{25.2}$$

In addition, the multiplicative expression for the transfer functions of (25.2) are resulted [35]:

$$G_1(s) = \frac{\delta_1}{d}(s) = \frac{(J_2 s^2 + b)}{(J_1 + J_2)s^2 * (J_c s^2 + b)} \; ; J_c = \frac{J_1 J_2}{J_1 + J_2}$$
$$G_2(s) = \frac{\delta_2}{d}(s) = \frac{b}{(J_1 + J_2)s^2 * (J_c s^2 + b)} \quad (26.2)$$

In which we deduce the following resonance and anti-resonance frequencies corresponded to the poles and zeroes of (26.2) as:

$$f_r = 0 \;\&\; \frac{1}{2\pi}\sqrt{\frac{b}{J_c}} \; [Hz]$$
$$f_a = \frac{1}{2\pi}\sqrt{\frac{b}{J_2}} \; [Hz] \quad (27.2)$$

As result, Based on (27.2), the Eigen frequency of inter-area oscillation are related to $J_c = \frac{J_1 J_2}{J_1 + J_2}$. Since the numerator of J_c is the product of multiplication despite the denominator as the product of summation, hence decrease of inertia either in both areas or just in one area resulting in lowering of J_c which in turn causes increase at the frequency of inter-area oscillation.

FIG. 13 shows the Bode-plot of the response of the two area power system based on derived transfer functions (26.2), resulting from the combination of the two mode responses. At $f = f_a$the transfer function shows an 'anti-resonance' according to the zero in the transfer function. At $f = f_r$ both areas will resonate while the dynamic of the first area is 180◦ out of phase with respect to the dynamic of the second area. When $f > f_r$ the slope of the Bode-plot of the first area will continue at -40 dB/dec while the second area does no longer join the dynamic of the first area since the slope of the response of the second area becomes twice as steep as the slope of the first area. Moreover, as illustrated in FIG. 14, by lowering the inertia, we can observe increasing on resonance frequency at both areas [30], [35].

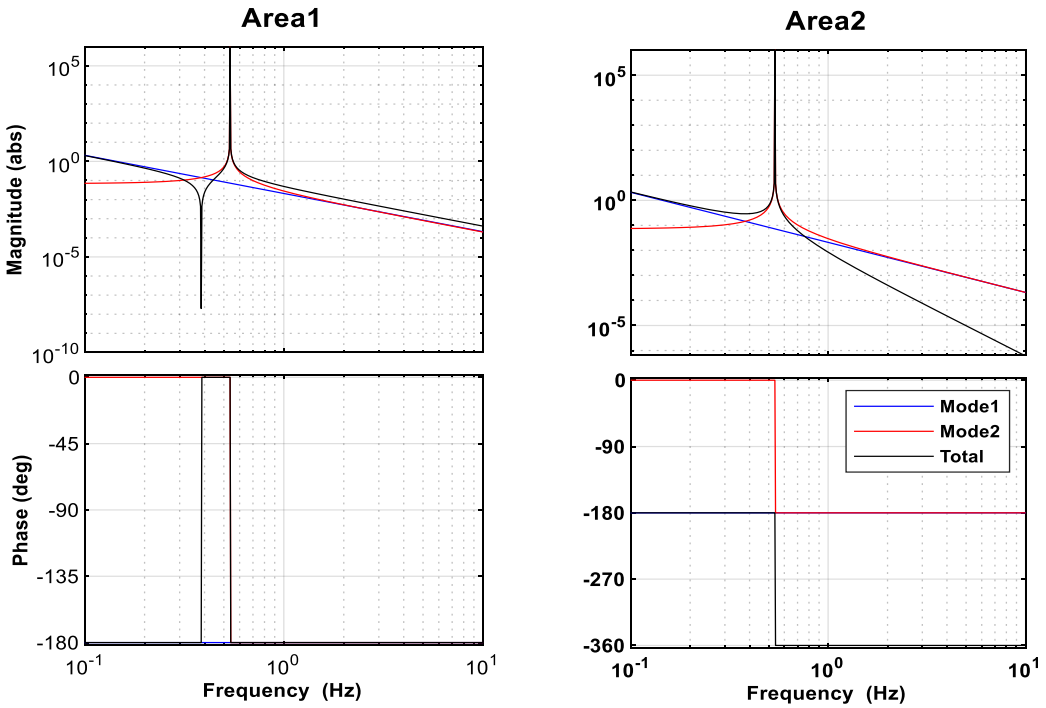

FIG. 13: Bode-plot of the response of the two area power system with J_1= 0.3104*2, J_2= 0.2948*2.

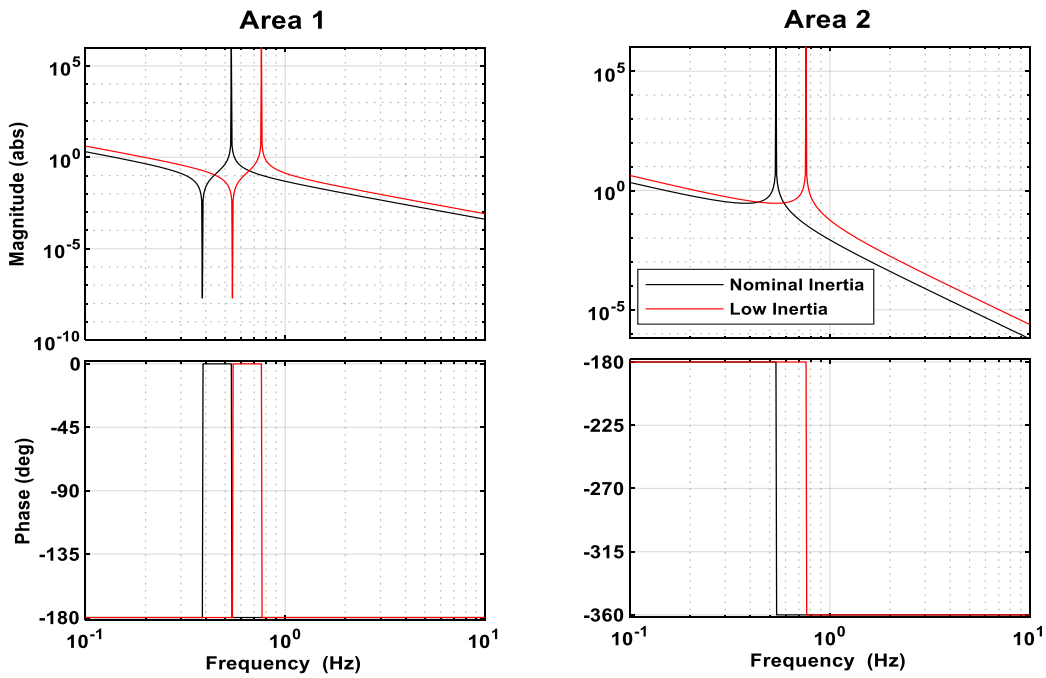

FIG. 14: Bode-plot of the response of the two area power system with low inertia J_1= 0.3104, J_2= 0.2948.

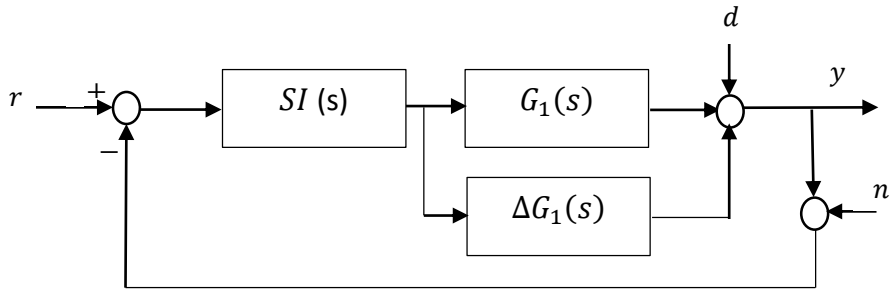

FIG. 15: Closed loop block diagram with considering measurement noise, output disturbances and parameter fluctuations [24], [25].

2.7 Synthetic Inertia and Power System Dynamics

The purpose of a synthetic inertia is to employ a fast primary control in order to compensate lack of physical inertia in low inertia power systems resulted from penetration of renewable energy sources. Based on the same discussion at last sections, the conventional primary controls, like prime mover controls, are not enough fast to maintain the frequency as well as the whole low inertia power system reliable against the high frequent disturbances (load-generation changes). Therefore, for instance the fast power electronic based devices can be applied to realize the synthetic inertia abstraction as fast primary control system [3].

The main concept of synthetic inertia is however based on the swing equation, the other algorithms such as droop-based or synchronous generator-based can be also considered to mimic the physical inertia effect. As the synthetic inertia algorithm is a closed loop control and a feedback signal is required to be measured hence some consideration, despite real inertia, related to feedback control including measurement delay, dead band, sensor noise or measurement errors and parameter fluctuations must be taken into account. In addition, if we realize the synthetic inertia through energy sources, like wind and solar sources, then we can just use it in case of frequency drop, contrary to realization through batteries which can act in both cases of frequency fall and rise. FIG. 15 presents closed loop block diagram with considering measurement noise and, output disturbances and parameter fluctuations.

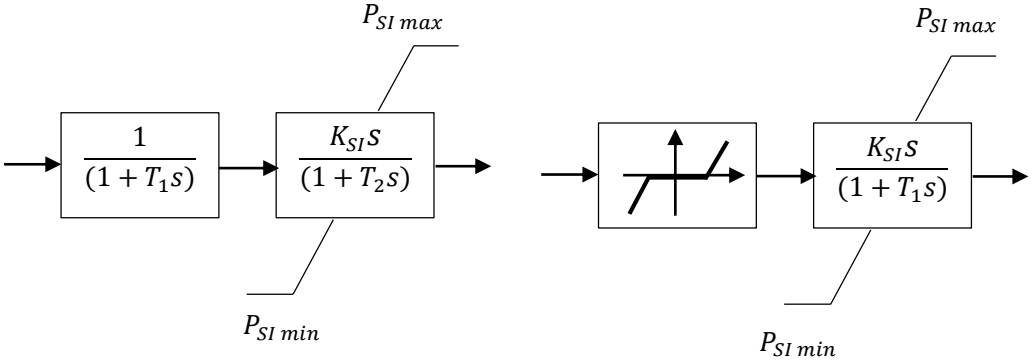

FIG. 16: Bock diagrams of Synthetic Inertia.

The swing equation based synthetic inertia can be derived as:

$$\Delta P_{SI,pu} = \frac{2H}{\omega_0}\frac{d\Delta\omega}{dt} = \frac{2H}{\omega_0}\frac{d^2\Delta\delta}{d^2t} = \frac{H}{\pi f_0}\frac{d^2\Delta\delta}{d^2t} = \frac{2H}{f_0}\frac{d\Delta f}{dt}$$
$$\frac{\Delta P_{SI,pu}}{\Delta f} = \frac{2H}{f_0}s = K_{SI,pu}s \qquad (28.2)$$
or
$$\frac{\Delta P_{SI,pu}}{\Delta\delta} = \frac{H}{\pi f_0}s^2 = K_{SI,pu}s^2$$

If we consider the delay of measurements and actuations or dead-band then we can model swing equation based synthetic inertia algorithm as presented at FIG. 16:

The values of delays can be from ten milliseconds up to several hundred milliseconds. The value of K_{SI} can be calculated as difference between equivalent inertia constants resulted from before and after penetration of renewable energy sources:

$$K_{SI} = \frac{2S_{base}}{f_0}(H_{eq,h} - H_{eq,l}) \qquad (29.2)$$

where $H_{eq,h}$ and $H_{eq,l}$ are the equivalent inertia constants of the area before and after contribution of low inertia energy sources in power system respectively.

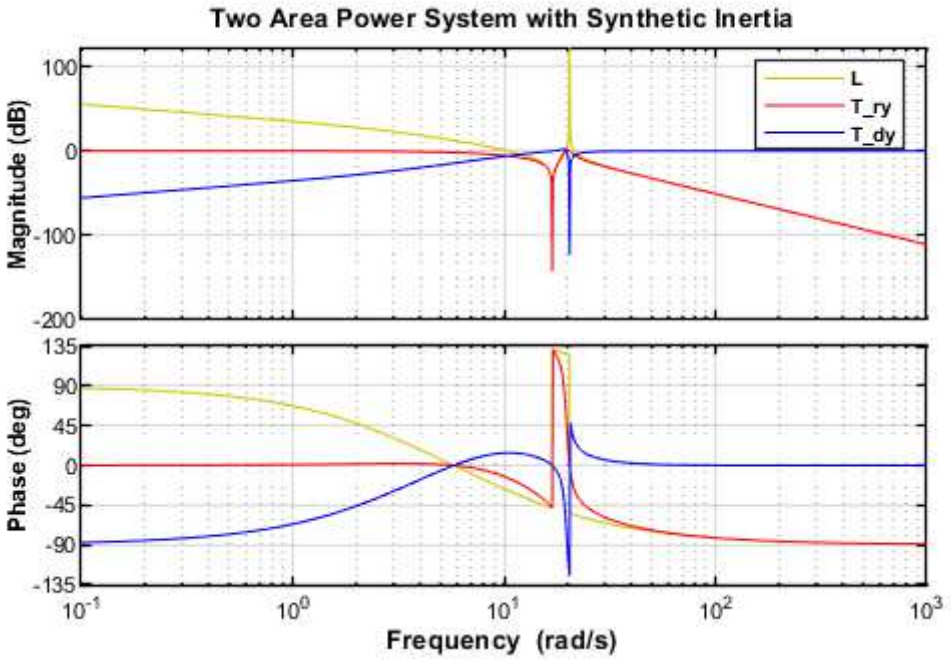

FIG. 17: This figure shows the frequency response of the open loop transfer function of (25.2) as well as closed loops transfer functions with respect to reference and disturbance signals by applying synthetic inertia [36]. $H\_1 = 6.5$; $H\_2 = 3$; $T\_1 = 0.1$; $T\_2 = 0.3$; $b = 10$;

The relevant transfer functions for closed loop system of FIG. 15 are [24], [25]:

$$L(s) = SI(s)G(s)$$

$$T_{r,y}(s) = \frac{L(s)}{1 + L(s)}$$

$$T_{d,y}(s) = \frac{1}{1 + L(s)}$$

By substituting (25.2) and (28.2) into the above formulations we can derive the open and closed loops transfer functions with respect to reference and disturbance signals as their frequency responses are illustrated in FIG. 17.

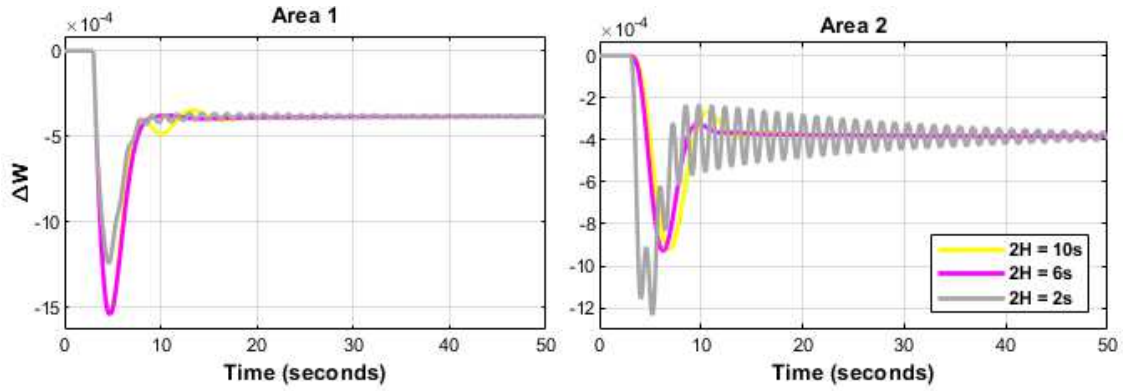

FIG. 18: This plot indicates the frequency response of a two area power system as the inertia constant for area 1 are kept constant 10s and for area 2 is decreased until 2s while the step load change is occurred at area 1 [37].

2.7 More Investigations with Two Area Power System

At this section we simulate the swing equation based dynamic model of the power system accompanied by first order dynamic model of turbine and governor as primary control system for each area [20]. We assume a closely coupled machines for each area and hence the values of inertia and damping coefficients are considered as equivalent amounts [20]. The model of each area consists of first order dynamic systems represent dynamics of power system, turbine and governor with droop feedback control [20]. The generating unit is a conventional reheat steam turbine used as well at section 2.3 which is faced with a step load change to model the small signal disturbance occurred at area 1 [20]. The original factors and the values of all parameters have been applied from [20]. However I modify some parameters in order to model the influence of other parts of the system like boiler and type of controls or mode of operation which can affect the system response and make it slower to some extent.

The power flow between two areas is modeled by the difference of rotor angles between two areas multiplied by a factor proportional to impedance of line connected the two areas [20].

The experiments are done by maintaining the value of inertia constant at area 1 the same and varying values of inertia constants at area 2.

FIG. 18 indicates the frequency response of both areas separately to the step load change at area 1. The experiments have been done by keeping the inertia at area 1 constant and equals to 10s while we changed the inertia of area 2 from 10 s to 2 s. As

shown, by lowering the inertia constant to 2s, in addition to higher RoCoF and frequency nadir the oscillatory behavior are resulted as well which is more remarkable at area 2 as area with lower inertia. This damped oscillatory behavior further shows the lack of primary control to overcome demand changes in right time at low inertia power systems.

The simulation results illustrate the notable different transient responses with respect to different inertia constants, although the steady state frequency deviation stays the same for all three values of inertia. The differences in transient responses are remarkable in the rate of frequency drop as well as nadir values.

2.8 Summary and Conclusion

In this chapter we mentioned the different models of power system with respect to inertia constant at various classes from single machine, single machine with infinite bus as well as multi-machine power system model. At each model we tried to formulate the effect of inertia constant on the dynamics of the system. We mentioned as well the some system metrics and disturbances as well as swing equation based algorithm of synthetic inertia.

We briefly discussed the future of power system with respect to inertia constant as well as showed the typical inertia constant for some various kinds of power generation unit which illustrated the significant drop of equivalent inertia constant at each synchronous area by penetration renewable energy sources like wind and solar energy sources. For instance most modern wind turbines are operated as variable speed wind turbines and interfaced through converters which completely decouples the inertia from the grid [38]. Obviously, PV and storage systems have also converters and inverters which do not contribute to the equivalent inertia constant in the synchronous areas [38].

We made an analogy between double mass spring system and two area power system in which the dynamics of two area power system was investigated in both time and frequency domains [34]. The frequency response and bode diagram was derived from external disturbances (generation or load variations) to generator phase angle to analyze the system dynamics in frequency domain in which the load damping coefficient

was neglected. The resonance and anti-resonance frequency of the system was formulated as a function of impedance between two areas and equivalent inertia constant as well.

The time domain investigation has been done based on simulation of the swing equation dynamic model of the power system accompanied by first order dynamic model of turbine and governor as primary control system for two area power system implemented in Matlab-simulink [20]. We assume a closely coupled machines for each area and hence we used the equivalent values for the parameters of inertia and damping coefficients. The simulation showed the effect of inertia constant to influence the some metrics of small signal transient frequency dynamics such as rate of change, frequency nadir as well as oscillatory behavior resulted due to low amount of moment of inertia in the system.

By modelling of introduced swing equation based of synthetic inertia, we considered the general challenges of implementation which all power converter based and feedback control systems facing with as follows [39]:

- Delays in measurement acquisition, signal processing and actuations.
- Constraints which there exist on currents, voltages and power of the elements

It will be investigating at next chapter how effective the derived synthetic inertia is on non-linear model of interconnected power system to improve the dynamics of low-inertia power systems [39].

3

3. PLACEMENT OF SYNTHETIC INERTIA

At the last chapter we investigated the performance of linearized low inertia power system with respect to small signal stability when the system is faced with load-generation variations and the parameters of the system change around their rated values. However inherently the power system is a nonlinear, hence at this chapter we are motivated to analyze the behavior of the system based on a nonlinear interconnected power system model [18].

At real power systems both manual (operator) and automatic controls are necessary to stabilize the system voltage and frequency around normal operating condition. These controllers are divided to different acting times which are categorized to primary, secondary and tertiary control actions [20], [22].

The automatic controls must be designed to ensure that oscillations decay over proper time. Oscillations, which are initiated by the normal small changes in load-generation, have the potential to involve in growing that in turn lead to cascade major disturbances and finally system collapse [40].

As the first realized systems to damp oscillations in primitive small scale interconnected power systems one can mention to amortiseur windings installed on the rotor of generators to produce a damping torque proportional to speed deviation [13], [40].

Along with getting larger and more complex power system as well as more emphasizing on the power system reliability, the other control systems from automatic voltage regulators and fast excitation systems to power system stabilizers, HVDC and FACTS are employed [13], [20], [40].

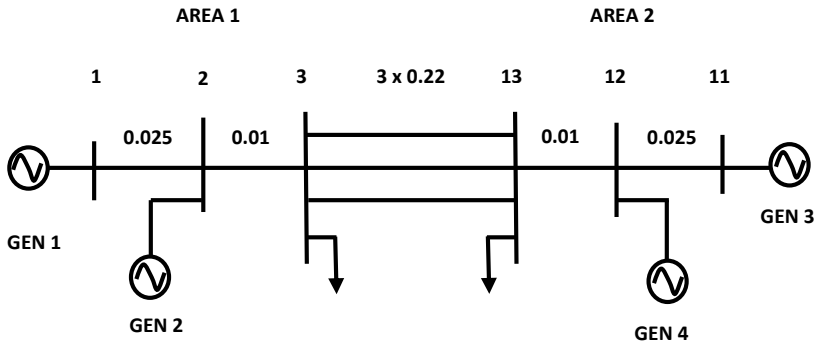

FIG. 19: Two area interconnected power system single line diagram (Original grid from Kundur (1993) [20].

Besides of all these controllers, as discussed before, the moment of inertia of the rotor shafts of the generators play a considerable role to keep the system stable at the first few seconds after happening a fault or a variation in the normal operating condition and before the primary controls take action [13], [40], [41]. This is a critical time period and as discussed earlier, the more the use of renewable resources, we have the higher decline in equivalent inertia which in turn makes this time period shorter and more critical.

Therefore, in this chapter, to do make entire investigation, I will discuss in three main sections as follows [39], [40]:

- Effect the lack of inertia on the nature of power system oscillations i.e. the power system without any controllers
- Effects the lack of inertia on the performance of power system accompanied with controllers such as governor and AVR
- Then I will evaluate the impact of synthetic inertia (as a fast response control solution) to show how effective it can make up the lack of generator's moment of inertia [39], [40].

All investigations are implemented within artificial model of two area interconnected power system shown in FIG. 19 implemented in Matlab/Simulink [39]. I will investigate employing of synthetic inertia accordingly on this nonlinear model [39], [40]. The two recommendable references, which I have utilized most for my investigations and analysis in this chapter, are, "System Norm Approaches for Power System Stability Analysis" by B. K. Poolla [3], and "Power System Oscillations" by G. Rogers [40].

3.1. Artificial Model of Two Area Interconnected Power System

FIG. 19 indicates the single line diagram of the system. The test system consists of two fully symmetrical areas linked together by two 230 kV lines of 220 km length. It was specifically designed in [20] to study low frequency electromechanical oscillations in large interconnected power systems as it mimics very closely the behavior of typical systems in actual operation. Each area is equipped with two identical round rotor generators rated 20 kV/900 MVA [23], [40], [42], [43].

The synchronous machines have identical parameters, except for inertia constants which are 6.5s in area 1 and 6.175s in area 2. The load is represented as constant impedances and split between the areas in such a way that area 1 is exporting about 400MW power to area 2. The reference load flow considered the slack machine in such that all generators are producing about 700MW [40], [42].

3.2 Effect the Lack of Inertia on the Nature of Power System Oscillations

To do this evaluation, I will do the simulations with identical detailed generators model without any controls. With applying no control in the system, obviously the field voltages and the mechanical torques stay constant during the simulation [40]. However, a damper winding on the direct axis and two on the quadrature axis of the generator produce torques proportional to speed deviation from its nominal value [40]. In order to excite a local mode without also exciting the inter area mode, an equal and opposite change in the mechanical torque on the generators in one area is applied [40]. Moreover, the inter-area mode can be excited by increasing the torque at one generator in area1 and decreasing the torque at a generator in area 2 [40].

I will investigate the influence of lack of moment of inertia on the speed of generators at both areas as well as the magnitude of terminal voltage at the tie bus 3 (the voltage at the sending end of the tie) and tie bus 13 (the voltage at the receiving end of the tie) as critical buses [13], [39], [40].

To this end, I will do the simulations in four general various cases:

1. Nominal constant of inertia in both areas.
2. Reduce constant of inertia in the area with occurred disturbance and keep the constant of inertia on the second area nominal.
3. Keep the total inertia in the area, which the disturbance is applied, nominal and decrease the total inertia on the other area without disturbance.
4. Decline inertia constant in both areas while the disturbance happened in just one area (area 1).

3.2.1 Nominal Inertia in both Areas ($H_1 = H_2 = Nominal$)

FIG. 20 shows the responses of the generator speeds to the above mentioned disturbance applied in area 1. Due to the torques which are produced proportional to speed deviation via damper windings, the amplitude of the local oscillations decays in initial steps of transient [40]. However, since there is no governor to control the speeds of the generators, the generators tend to accelerate (or decelerate) over the time. The generators in area 1 are in antiphase and oscillate against each other that in turn illustrate the domination of local mode in area 1, while the generators in area 2 oscillate without any phase shift [40]. The reduction in average tie bus voltages are also illustrated in (FIG. 21), as the speed deviations in both areas tends to increase [40].

3.2.2 Low Inertia in One Area ($H_1 < H_2$ *or* $H_2 < H_1$)

I will decrease the total inertia of area 1 from the nominal value by replacing a generator with a constant power source to model a low-inertia scenario in area 1 (FIG. 22-a) [3].

The simulation will be done again by applying a change in the mechanical torque on the generator in area 1 [3], [40]. As result, we observe an increase in frequency of oscillations at both areas as well as higher rate of change of rotor speeds. However the rise of acceleration in area 1 is significantly higher than area 2.

We can also see an extreme drop in voltages initially on both sending and receiving tie-line buses which is followed by loss of synchronicity (FIG. 23), despite monotonic voltages reduction represented in the previous section.

- Nominal Inertia in both Areas / without Controller

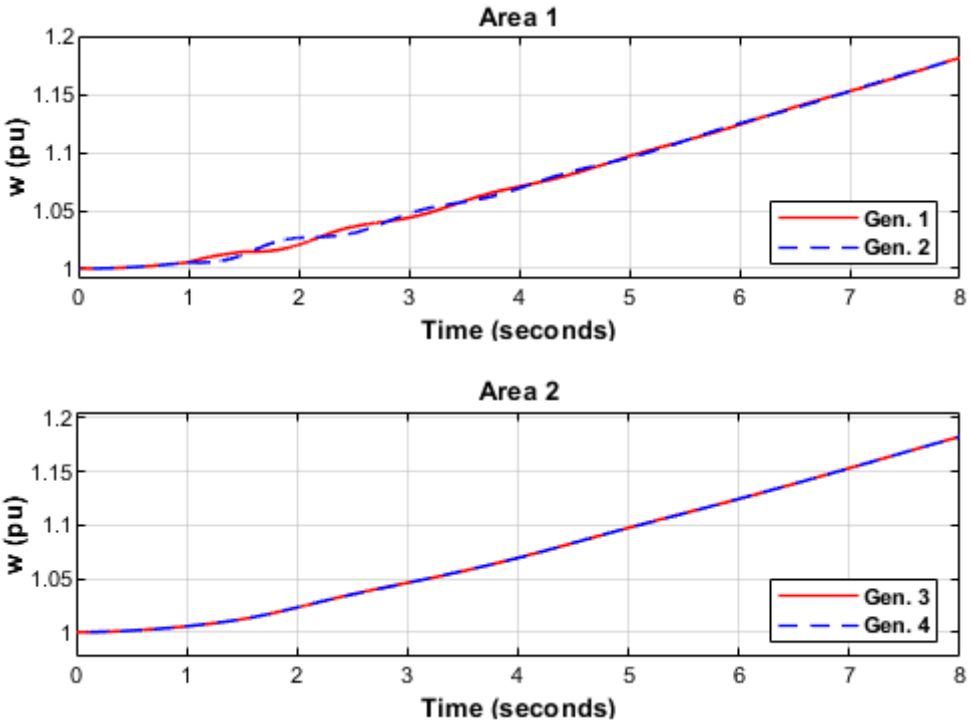

FIG. 20: Responses of generator speeds to disturbances applied in mechanical torques in generators in area 1 with nominal constant inertia (detailed generators model/without control).

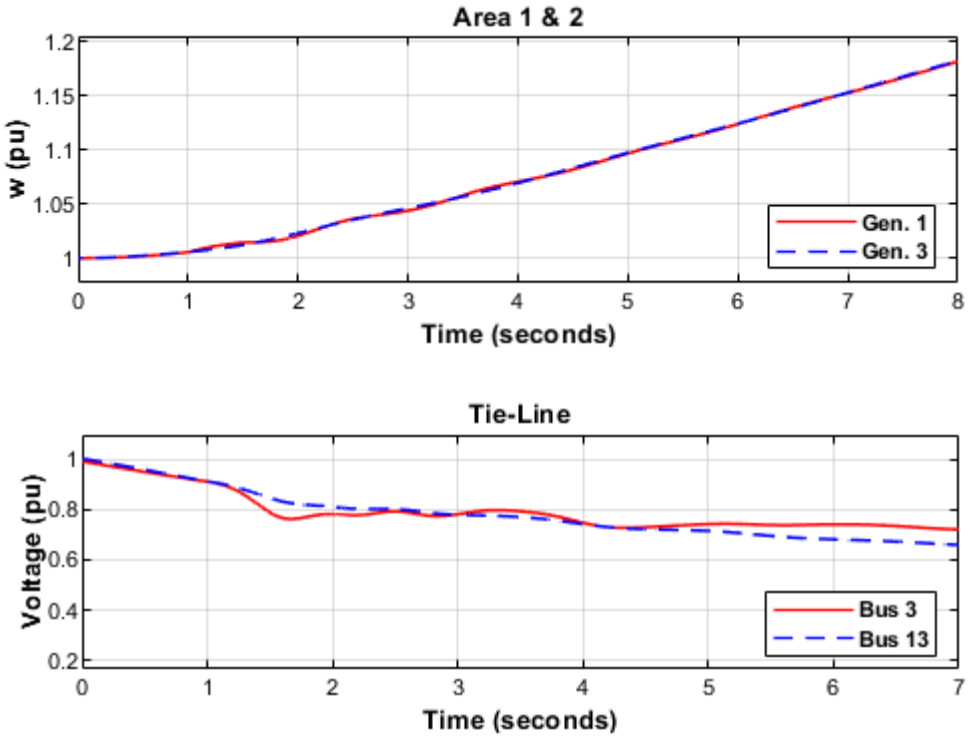

FIG. 21: Responses of generator speeds and voltage of bus 3 and 13 to disturbances applied in mechanical torques in generators in area 1 (detailed generators model/without control/nominal inertia in area 1 & 2) [40].

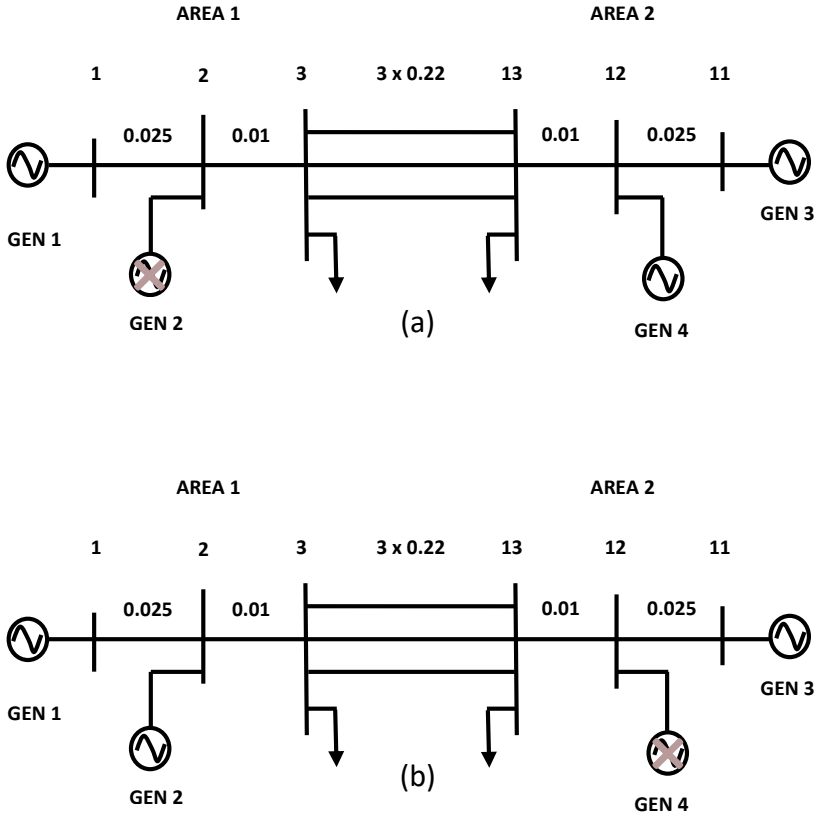

FIG. 22: Two area interconnected power system single line diagram. The crossed out generators are replaced by constant power source to mimic a low inertia scenario.

Although, this violent drop in tie-line bus voltages is happened due to the generators are uncontrolled, but as we will see in the next sections it will be also very problematic to control them via even exciting control systems.

By reducing the inertia of area 2 (which receives active power from area 1), the speed of generator at area 2 however oscillates in higher frequency, the rate of change stays the same for both areas. In this case the voltages drop within a longer time (FIG. 24).

3.2.3 Low Inertia in both Areas ($\boldsymbol{H_1 = H_2 = \frac{1}{2} * Nominal\ Value}$)

As indicated in FIG. 26, in this case, initially both generator speeds and tie bus voltages oscillate at approximately same frequency but they are in anti-phase and oscillate against each other [40].

- Low Inertia in Area 1 / without Controller

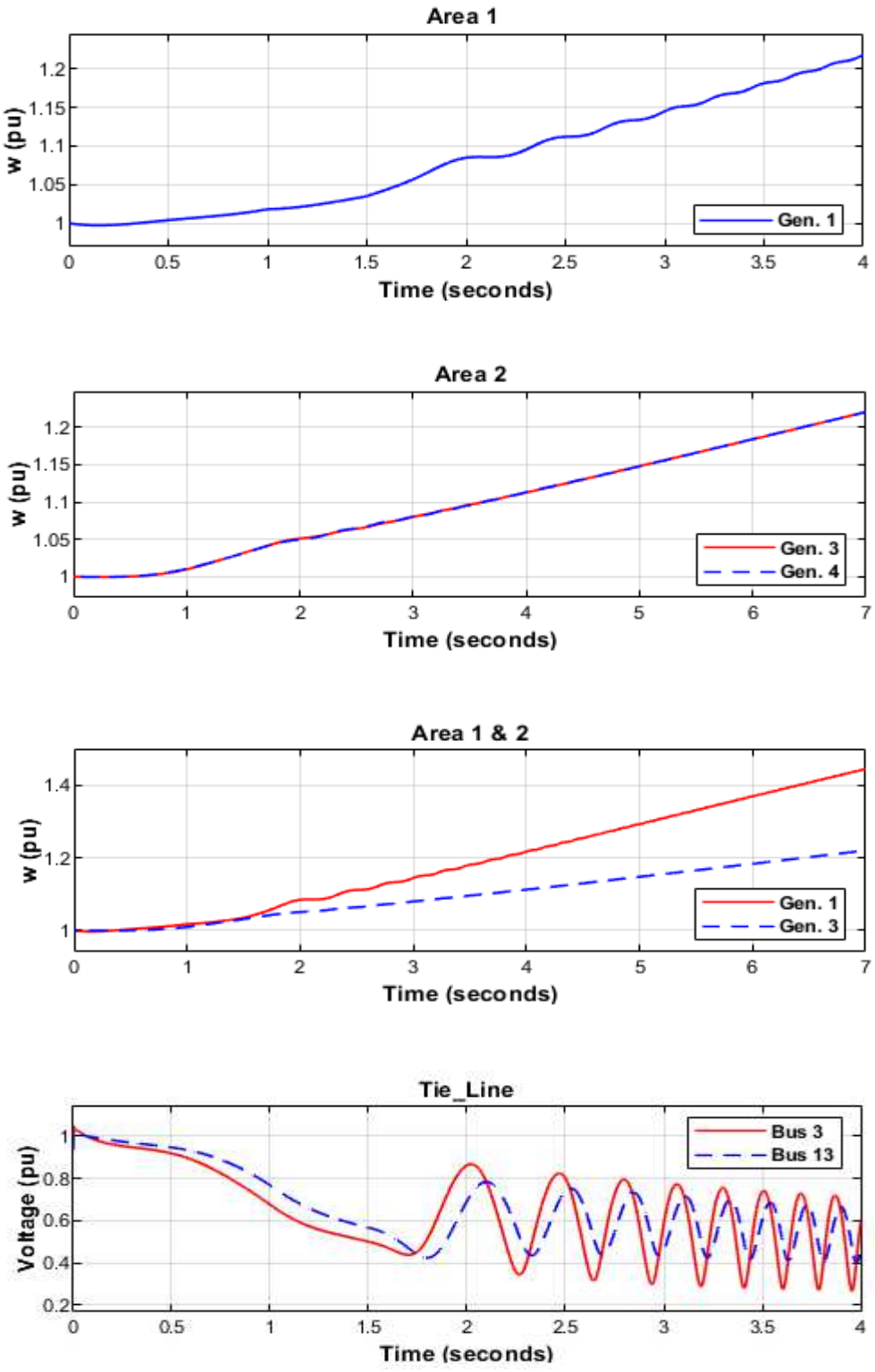

FIG. 23: Responses of generator speeds and voltage of bus 3 and 13 to disturbances applied in mechanical torque in generator in area 1 (detailed generators model/without control/reduced inertia area 1/ nominal inertia in area 2) [40].

After some seconds the speed of generator in area 2 accelerate more than one in area 1. This is because we have more drop in voltage at tie bus 13 that in turn causes more decrease in the electromagnetic torque [40]. The bus voltages (load buses 3 and 13) represent a very small drops at the beginning. But they fall dramatically after around 4 seconds that is completely different at the same simulation time in nominal inertia case, (FIG. 26).

- Low Inertia in Area 2 / without Controller

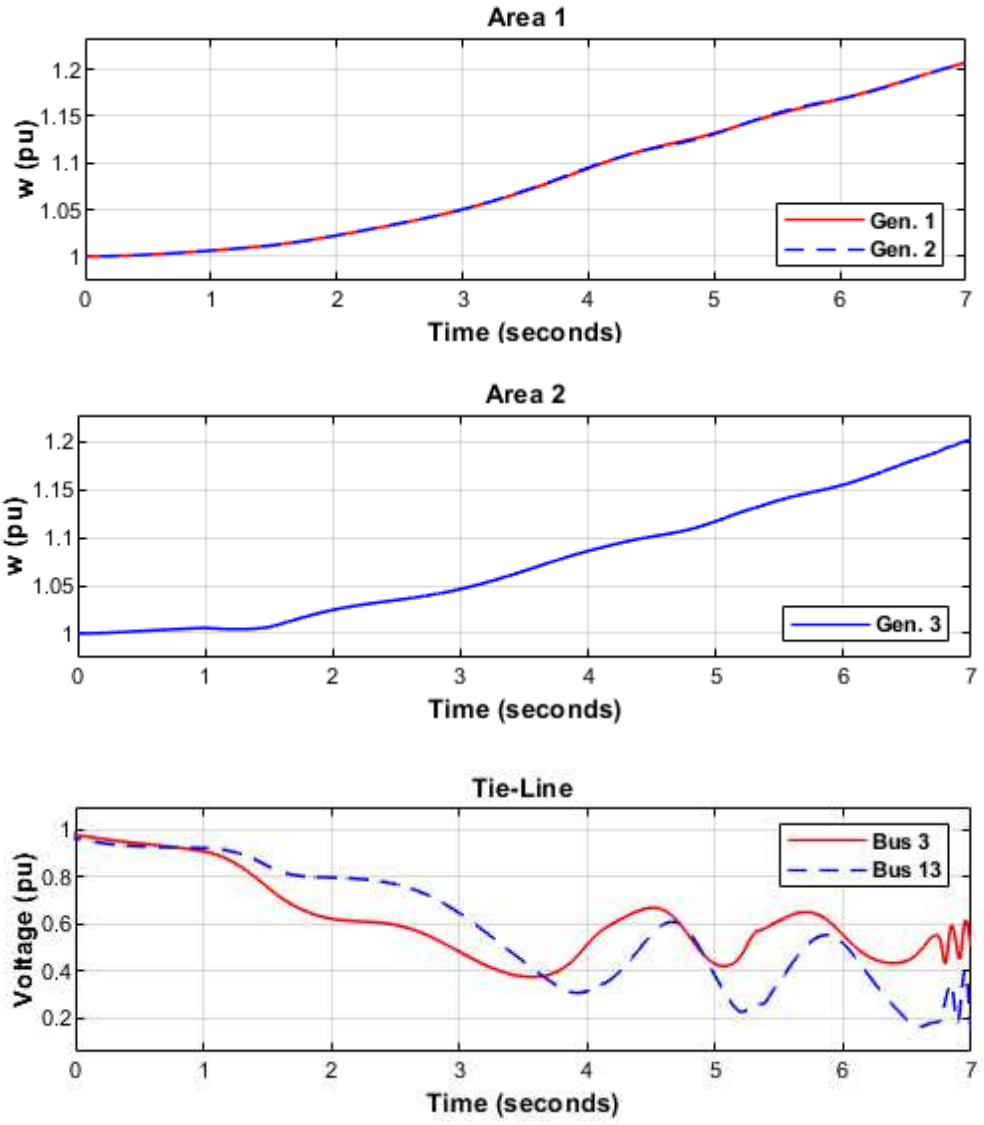

FIG. 24: Responses of generator speeds and voltage of bus 3 and 13 to disturbance applied in mechanical torque in generator at area 1 (detailed generators model/without control/reduced inertia area 2/ nominal inertia in area 1) [40].

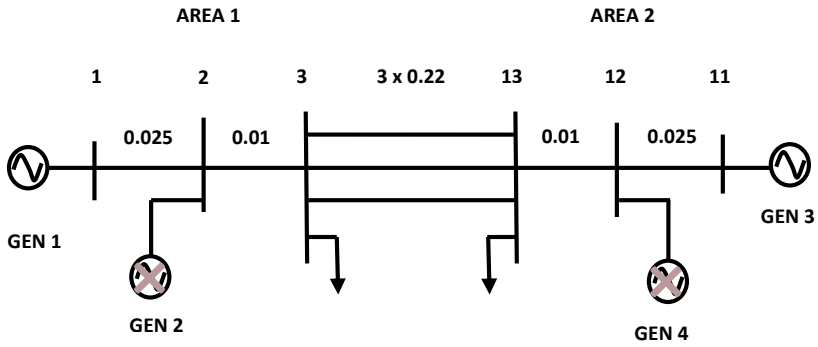

FIG. 25: Two area interconnected power system single line diagram. The crossed out generators are replaced by constant power source to simulate a low inertia scenario [3] [40].

- Low Inertia in both Areas / without Controller

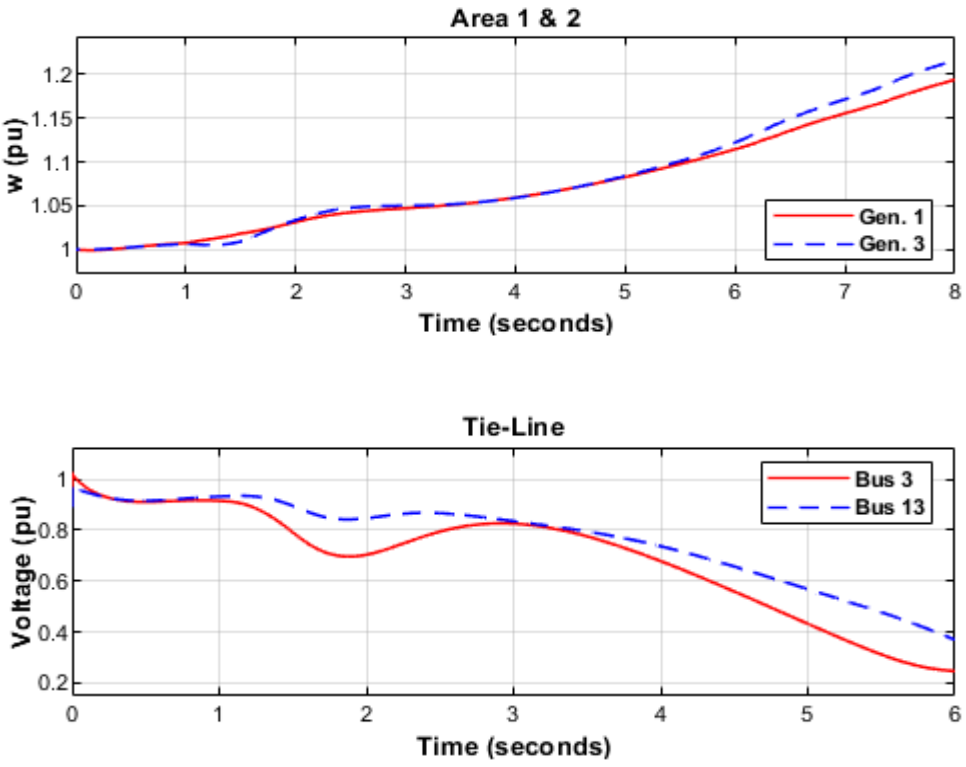

FIG. 26: Responses of generator speeds and voltage of bus 3 and 13 to disturbance applied in mechanical torque in generator at area 1 (detailed generators model/without control/reduced inertia both area 1 and 2) [40].

As it is clearly observable in the previous three simulations, we see almost completely different frequency and voltage responses of an interconnected power system as we have different value of inertia which indicates the significant effect of this parameter on dynamics of the system.

Interestingly, the behavior of the frequencies and voltages of the system are different if we have the equal inertia in both areas but lower in comparison to the case which we have equal and higher values. In the other word, not only the unbalancing of inertia in two areas has intense influence on the system dynamics, but also decreasing the inertia however this reduction be the same in two areas, effects the system dynamic significantly.

Table 3 summarizes the results of the above four experiments done for the two area power system without controller to show the effects of low total inertia on the nature of power system dynamics.

Condition	**Gen. Speed**				**Tie-Line Voltage**			
	Frequency of Oscillation compared to Nominal Case		Rate of Change		Frequency of Oscillation compared to Nominal Case		Rate of Change	
	Area 1	Area 2	Area 1	Area 2	Sending End	Receiving End	Sending End	Receiving End
Nominal Inertia Both Areas	-	-	0.02	0.02	-	-	-0.1	-0.1
Low Inertia Area 1	Higher	Same	0.05	0.03	Loss of Synchronicity after 1.5s		-0.27	-0.2
Low Inertia Area 2	Lower	Higher	0.03	0.03	Loss of Synchronicity after 3.5s		-0.14	-0.12
Low Inertia both Areas	Lower	Higher	0.025	0.027	Lower	Higher	-0.13	-0.06

Table 3: The summery of the results of experiments for the case of two area power system without controller.

At the next section it will be also shown that in case, which we have the controllers such as governors and automatic voltage regulators, the effect of varying of inertia in different forms, like the location and the value, will be considerable in system dynamics and stability point of views.

3.3 Controlled Detailed Generator Model

This simulation is comprised power system generators equipped with governor and AVR controllers which the speeds are held close to nominal speed by means of governors and the system voltages remain close to their reference levels via the automatic voltage regulators [40].

The purpose of this part is to show how decline of inertia, due to emulation of renewable energy sources, effects an interconnected power system (i.e. in our case two-area interconnected power system) in term of small signal stability with considering this issue that the generators are equipped just with governors and AVR controllers and no synthetic inertia is applied on the system [23], [40], [44]. Hence, I will decrease the inertia in area 1 by replacing again one generator with constant power source [3].

FIG. 27 and FIG. 28 illustrate the dynamics of declined inertia power system before and after applying 200MW load increase [3], as disturbance in area 1, respectively.

Although we have the governor and automatic voltage regulator in the system, but we observe an oscillations with higher frequency and amplitude and with lower damping ratio as well as high rate of change of frequency (RoCoF) and high frequency nadir in all generators in both areas at initial times when we have the disturbance on the system [3], [40].

Comparing the dynamics of grid frequency and tie-line voltages, before and after occurring the fault in the system, we observe a significant drop of frequency as well as tie-line voltage at bus 13 in area 2 which receives energy from area 1 [40]. These drops in frequency and voltages are notable which in turn show the inefficient performance of traditional primary control actions against the variation of load in the hybrid power systems in which the total inertia is declined remarkably.

- Low Inertia in Area 2 / with Controller / with Disturbance

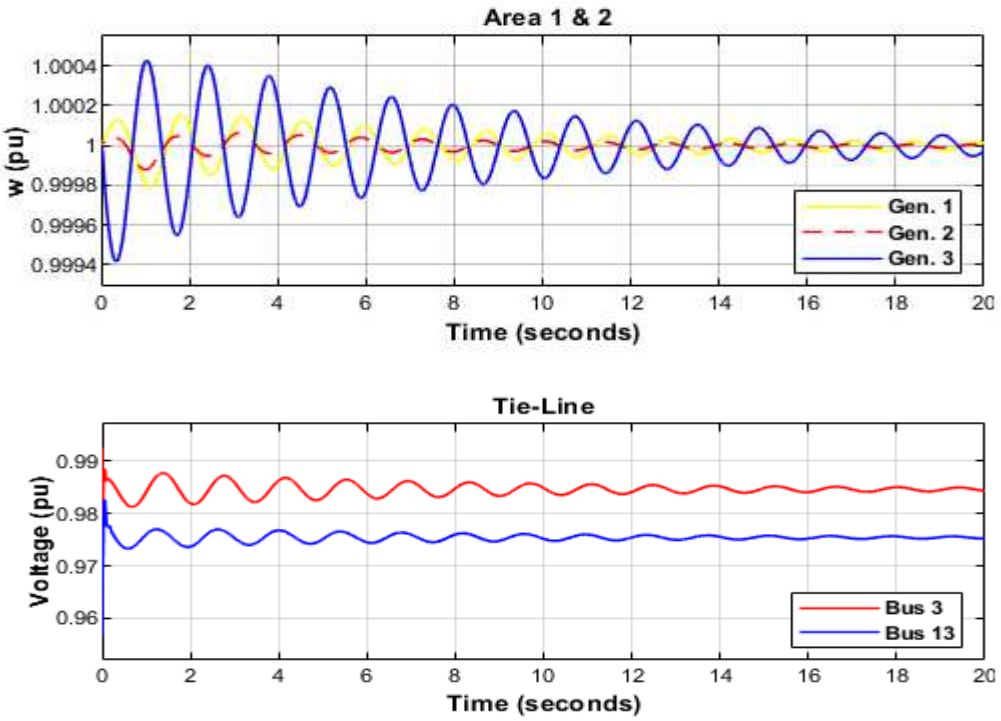

FIG. 27: Generator speeds and voltages of tie buses (detailed generators model/with control/without PSS/without SI/without disturbance).

- Low Inertia in Area 2 / with Controller / without Disturbance

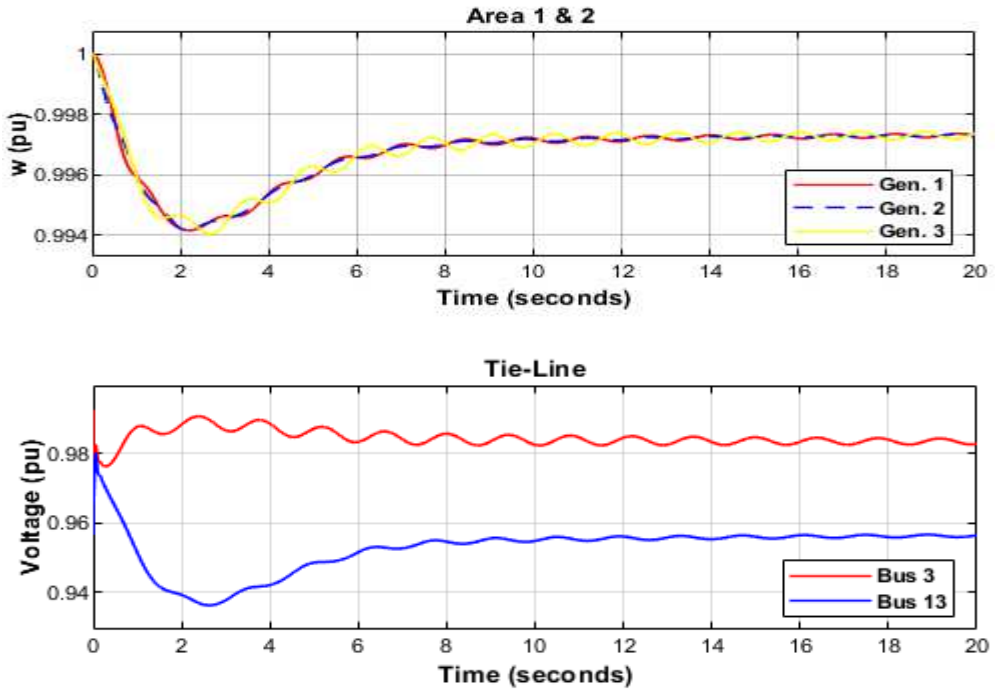

FIG. 28: Responses of generator speeds and voltage of tie buses to a 200MW increased load in area 1 with reduced inertia at area 2 and nominal inertia at area 1 (detailed generators model/with control/without SI/with disturbance).

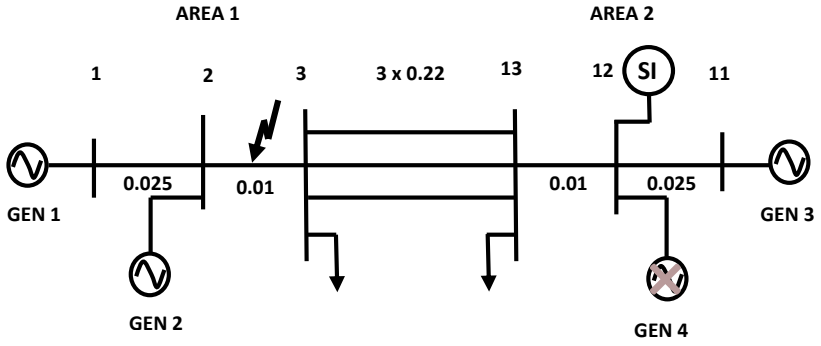

FIG. 29: Two area interconnected power system single line diagram. The crossed out generator is replaced by constant power source to simulate a low inertia area, while the black lightning symbol indicates the occurrence place of disturbance. The synthetic inertia is demonstrated via the symbol SI [3] [22] [41].

3.4 Allocation of synthetic inertia

At this section, I utilize synthetic inertia on power system with low inertia due to the loss of synchronous machines. The general approach at this section is based on applying synthetic inertia as a fast primary control action to a low inertia power system simulated by replacing synchronous machine with constant power source and investigating its effects after occurring a small signal disturbance [3], [22], [39].

AS mentioned, the problem of placing the synthetic inertia has been investigated for small-scale test case of two area interconnected power system with nonlinear detailed generator models based on time-domain system responses such as rotor speed of the generators and tie bus voltages. In order to model low inertia power system, we reduced the equivalent inertia at area 2, which receives energy from area 1, by substituting one synchronous generator with no inertia power source as well as allocating synthetic inertia at area 2 while we increase the load in area 1 to simulate small signal disturbance [3], [22].

As discussed in the previous chapter, the concept of synthetic inertia control law device is based on injecting active power proportional to rate of change of frequency. By, for instance, a phase-locked loop which is synchronized to a bus voltage we can estimate the bus voltage phase angle, the frequency as well as the rate of change of frequency so we can model the synthetic inertia device as [3]:

$$P_{SI,i} = K_{SI,i}\dot{f}_i$$

where $P_{SI,i}$is the power injected in bus i with gain, $K_{SI,i}$, and rate of change of frequency at related bus, $\dot{f}_i$, [3], [22].

The assessment is done with detailed analysis for 200MW step load rise as disturbance happened on area 1 with reducing the inertia at area 2 in almost half by replacing generator 4 with constant power source, while the area 1 remains the same in total inertia constant and without happening any disturbance in area 2 as well (FIG. 29) [3].

Moreover, I employ the synthetic inertia in area 2 with the gain equals to the value of reduced inertia constant at area 2 based on equation (29.2).

FIG. 30 shows the results of the simulation explained above for the generator speeds of both areas 1 and 2, voltages of tie buses as well as the active power flow through the tie-line from area 1 to area 2.

Through comparing FIG. 30 and FIG. 28, we can observe the response of the mentioned system parameters before and after employing of synthetic inertia respectively which illustrates that the concept of synthetic inertia can improve sufficiently the dynamic of system parameters like frequency, voltages of tie-line as well as the power flow between the interconnected areas in terms of rate of change of frequency, frequency nadir, damping ratio as well as local and inter-area frequency and amplitude of oscillations.

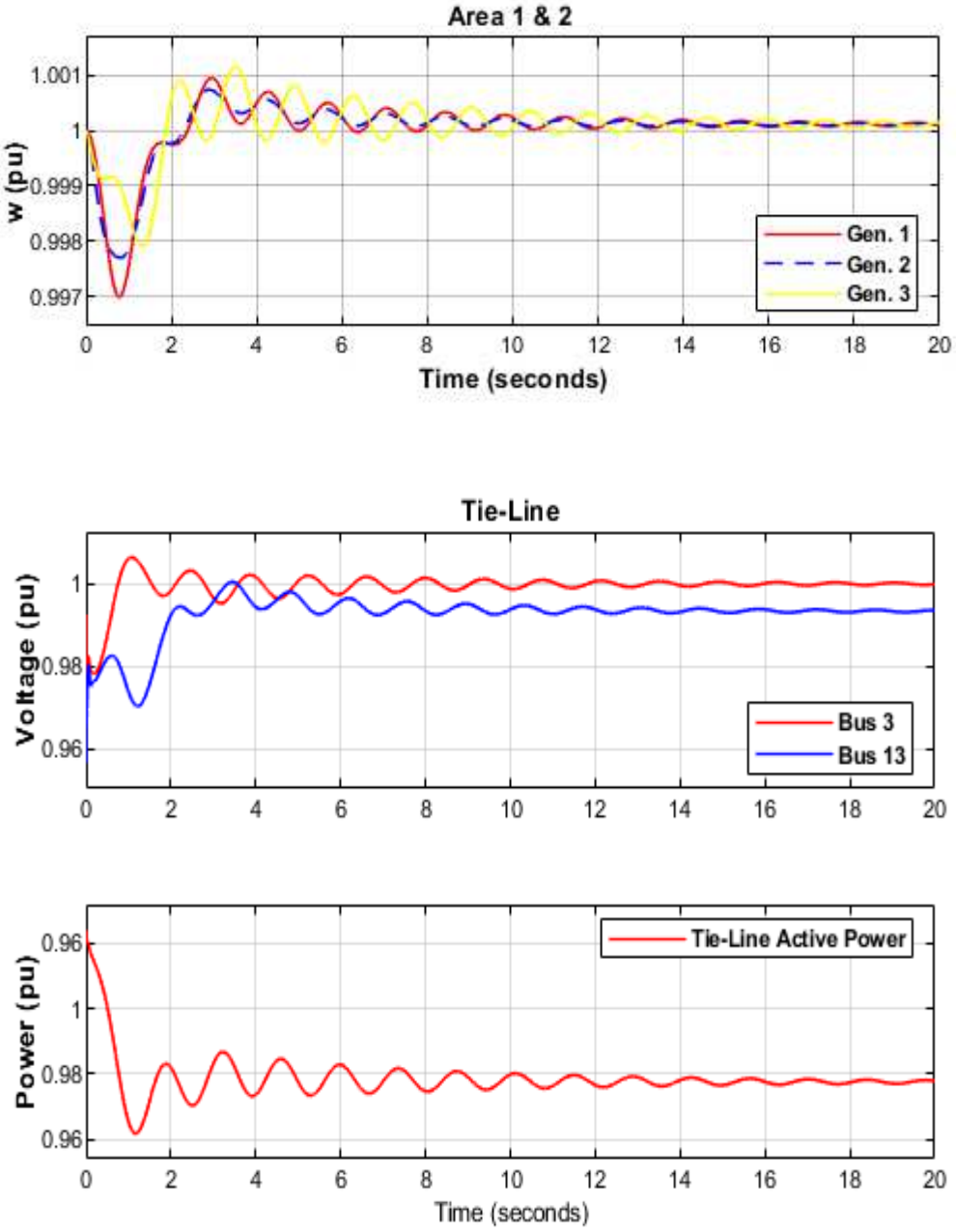

FIG. 30: Responses of generator speeds and voltage of tie buses to a 200MW increased load in area 1 with reduced inertia at area2 and nominal inertia at area1 (detailed generators model/with control/with employing SI and differentiating action in areas 1).

4

4. SUMMARY AND CONCLUSION

In this work we considered the problem of small signal stability, i.e. rotor angle and frequency stability, of power systems influenced by penetration of renewable energy sources. As discussed in details, the more permeation of low- and no-inertia energy sources like, wind and solar power plants, the more dynamic will be the power system so that the necessity of faster control reserve will be more vital. In scope of this thesis we investigated a possible control law i.e. synthetic inertia as it represents a feedback control strategy proportional to derivate of frequency of the grid. In order to do make entire investigation, I discussed an interconnected power system in three following aspects:

1. Effect the lack of inertia on the nature of power system oscillations i.e. the power system without any controllers.
2. Effects the lack of inertia on the performance of power system accompanied with controllers such as governor and AVR.
3. Then I evaluated the impact of synthetic inertia (as a fast response control solution) to show how effective it can make up the lack of generator's moment of inertia in hybrid power systems.

All investigations have been done within a linear as well as a non-linear artificial model of two area interconnected power system in which I investigated employing the concept of synthetic inertia (as a fast response control solution) accordingly.

We investigated the effect of lack of moment of inertia on the local and inter-area parameters as well as the magnitude of terminal voltage at the sending and receiving ends of the tie-line as critical buses.

We compared the simulations in four general various cases:

1. Considered Nominal constant of inertia in both areas.
2. Reduced constant of inertia in the area with disturbance and kept the inertia constant on the second area nominal.
3. Kept the constant of inertia in the area with the disturbance nominal, while decreased the inertia on the other area without disturbance.
4. Declined constant of inertia in both areas while the disturbance happened in just area 1 which is exporting power to area 2.

As we showed decreasing of the inertia has sufficient effect on the local and inter-area parameters such as frequency and the magnitude of terminal voltages at both end of tie-line so that we observed the loss of synchronicity in the case that we have no control in the system at all.

Moreover, in case of applying governor and automatic voltage regulator in the system, we observed high frequency and amplitude of oscillations with very low damping, as well as high rate of change of frequency (RoCoF) in all generators in both areas at initial times of transient when the inertia in the system is reduced. In addition, they converted to negative damped oscillations when we applied the disturbance on the system.

These negative damped oscillations behavior in tie bus voltages in turn shows the inefficient action of automatic voltage regulators over the time to overcome the problem.

Additionally, the simulation results illustrated that interconnected power system shows different dynamic behaviors dependent on which sending or receiving area is considered as low inertia area.

Finally, by utilizing synthetic inertia in the area with low inertia the simulations illustrated that the concept of synthetic inertia can improve sufficiently the dynamic of system parameters like frequency, voltages of tie-line as well as the power flow between the interconnected areas.

In this work we adjusted a constant amount of synthetic inertia exactly equals to the amount of inertia which we lost in power system however in the real integrated power systems the amount of inertia is a time-variant parameter and it changes with the

amount of generated energy by renewable sources which in turn are dependent on the environment conditions, the velocity of wind, the time of day, the season, etc. Hence in order to cover this problem to prevent making any instability in the system due to injection of insufficient feedback control effort as well as optimizing the energy of controller, the design of controller based on model predictive control (MPC) algorithm can be utilized which will be considered in my future work and investigations.

5. Bibliography

[1] M. Anvari , L. . R. Gorjão und M. Timme, „Stochastic properties of the frequency dynamics in real and synthetic power grids," *American Physical Society,* 2020.

[2] H. Saberi, S. Mehraeen und M. . M. Rezvani, „Intelligent Operation of Small-Scale Interconnected DC Grids via Measurement Redundancy," *IEEE Transactions on Industrial Electronics ,* Bde. %1 von %21-1, Nr. 10.1109/TIE.2019.2914623, p. PP(99), 2019.

[3] B. K. Poolla, System Norm Approaches for Power System Stability Analysis, ETH Library, 2019.

[4] „iea.org," March 2019. [Online]. Available: https://www.iea.org/reports/global-energy-co2-status-report-2019/emissions. [Zugriff am September 2020].

[5] „BP Statistical Review, 68th edition," 2019. [Online]. Available: https://www.bp.com/content/dam/bp/business-sites/en/global/corporate/pdfs/energy-economics/statistical-review/bp-stats-review-2019-full-report.pdf. [Zugriff am September 2020].

[6] REN21, „Renewables 2012 global status report," REN21, www.ren21.net , 2018.

[7] „gatesnotes," [Online]. Available: https://www.gatesnotes.com/Climate-and-Energy. [Zugriff am 2020].

[8] A. B. Lovins und Rocky Mountain Institute, Reinventing Fire: Bold Business Solutions for the New Energy Era a book, Chelsea Green Publishing, 2011.

[9] L. B. A. I. t. P. b. Blogger., „https://lukebutcher.blogspot.com," 27 November 2013. [Online]. Available: https://lukebutcher.blogspot.com/2013/11/. [Zugriff am September 2020].

[10] „iea.org," 11 February 2020. [Online]. Available: https://www.iea.org/articles/global-co2-emissions-in-2019. [Zugriff am September 2020].

[11] „International Renewable Energy Agency," 2018. [Online]. Available: https://www.irena.org/media/Files/IRENA/Agency/Publication/2018/Apr/IRENA_Report_GET_2018.pdf. [Zugriff am April 2020].

[12] „Powerweb," FORECAST INTERNATIONAL, [Online]. Available: http://www.fi-powerweb.com/Renewable-Energy.html. [Zugriff am April 2020].

[13] A. Ulbig, T. S. Borsche und G. Andersson, „Impact of Low Rotational Inertia on Power System Stability and Operation," *arXiv.org,* Nr. arXiv:1312.6435v4 [math.OC], 22 Dec 2014.

[14] „Weather Underground," TWC Product and Technology LLC, [Online]. Available: https://www.wunderground.com/history/daily/at/fischamend/LOWW/date/2020-3-24. [Zugriff am 2020].

[15] I. E. Agency, „Digitalisation and Energy," November 2017. [Online]. Available: https://www.iea.org/reports/digitalisation-and-energy#fundamentally-transforming-electricity-via-digitally-interconnected-systems. [Zugriff am April 2020].

[16] ENTSO-E, „Scenario Outlook&Adequacy Forecast 2015," ENTSO-E, 2015.

[17] ENTSO-E, „Operation Handbook," 2009. [Online]. Available: www.entsoe.eu/resources/publications/entso-e/ operation-handbook/. [Zugriff am April 2020].

[18] . J. kumar, . P. kumar, A. Mahesh und A. Shrivastava, „Power System Stabilizer Based On Artificial Neural Network," *IEEE,* Nr. 0.1109/ICPES.2011.6156656, 2011.

[19] F. Milano, F. Dörfler und G. Hug, „Foundations and Challenges of Low-Inertia Systems," in *Conference: Power Systems Computation Conference (PSCC)*, Dublin, Ireland, 2018.

[20] P. Kundur, Power system stability and control, New York: McGraw-Hill Inc, 1994.

[21] H. Thiesen, C. Jauch und A. Gloe, „Design of a System Substituting Today's InherentInertia in the European ContinentalSynchronous Area," *Energies,* Nr. 10.3390/en9080582, 2016.

[22] Bala Kameshwar Poolla, Dominic Groß und Florian Dorfler, „Placement and Implementation of Grid-Forming and Grid-Following Virtual Inertia and Fast Frequency Response," *math.OC,* Nr. arXiv:1807.01942v4 , 9 Jan 2019.

[23] Ravi Shankar, Ravi Bhushan und Kalyan Chatterjee, „Small-signal stability analysis for two-area interconnected power system with load frequency controller in coordination with FACTS and energy storage device," *Ain Shams Engineering Journal 7(2):603-612,* Nr. 10.1016/j.asej.2015.06.009, August 2015.

[24] A.Kugi, „Vorlesung und Übung Automatisierung," *Institut für Automatisierungs- und Regelungstechnik, TU Wien,* 2019-2020.

[25] A. Kugi, Vorlesung und Übung Automatisierung, Institut für Automatisierungs- und Regelungstechnik, TU Wien, Wintersemester 2014/2015.

[26] Panagiota Fokianou, Maria Samarakou, Dionisis Kandris und Emmanouil D. Fylladitakis, „Star-Delta Switches Evaluation for Use in Grid-Connected Wind Farm Installations," *Hindawi Publishing Corporation,* Nr. 10.1155/2013, 2014.

[27] K. N. Bangash, M. E. A. Farrag und A. H. Osman, „Investigation of Energy Storage Batteries in Stability Enforcement of Low Inertia Active Distribution Network," *Springer,* 2019.

[28] D. P. Kothari und I. Nagrath, Modern power system analysis, Tata, McGraw-Hill Education, 2011.

[29] Jan Machowski, Zbigniew Lubosny, Janusz W. Bialek und James R. Bumby, Power System Dynamics: Stability and Control, ISBN: 978-1-119-52634-6 .

[30] ENTSO-E, WindEurope, SolarPower Europe und T&D EUROPE, „High Penetration of Power Electronic Interfaced Power Sources and the Potential Contribution of Grid Forming Converters".

[31] ENTSO-E, „Guidance document for national implementation for network codes on grid connection High Penetration of Power Electronic Interfaced Power Sources (HPoPEIPS)," 29 March 2017 .

[32] P. W. Sauer und M. A. Pai, Power System Dynamics and Stability, Prentice Hall, 1998.

[33] Mohammad Pirani, Ehsan Hashemi, Baris Fidan und John W. Simpson-Porco, „H∞ Performance of Mechanical and Power," Nr. 10.1016/j.ifacol.2017.08.453 .

[34] Nizamuddin Hakimuddin, Anita Khosla und Jitendra Kumar Garg, „Centralized and decentralized AGC schemes in 2-area interconnected power system considering multi source power plants in each area," *Elsevier B.V. on behalf of King Saud University,* Nr. N. Hakimuddin et al./Journal of King Saud University – Engineering Sciences 32 (2020) 123–132, 2018.

[35] Robert Munnig Schmidt, Georg Schitter, Adrian Rankers und Jan van Eijk, The Design of High Performance Mechatronics, ISBN 978-1-64368-050-7 (print) | 978-1-64368-051, 3rd Revised Edition.

[36] Saeed Golestan, Mohammad Monfared, Francisco D. Freijedo und Josep M. Guerrero, „Performance Improvement of a Prefiltered Synchronous-Reference-Frame PLL by Using a PID-Type Loop Filter," *IEEE TRANSACTIONS ON INDUSTRIAL ELECTRONICS,* Bde. %1 von %2VOL. 61, NO. 7, Nr. 10.1109/TIE.2013.2282607, 2014.

[37] Weichao Zhang, Xiangwu Yan und Hanyan Huang, „Performance Tuning for Power Electronic Interfaces Under VSG Control," *Applied Sciences 10(3):953,* Nr. 10.3390/app10030953, 2020.

[38] Francisco Gonzalez-Longatt, Edward Chikuni und Emanuel Rashayi, „Effects of the Synthetic Inertia from wind power on the total system inertia after a frequency disturbance," in *Industrial Technology (ICIT), 2013 IEEE International*, February 2013.

[39] V. JEYALAKSHMI und P. SUBBURAJ, „Load frequency control in two area multi units Interconnected Power System using Multi objective Genetic Algorithm," *WSEAS TRANSACTIONS on POWER SYSTEMS,* Bd. Volume 10, Nr. E-ISSN: 2224-350X, 2015.

[40] G. Rogers, Power System Oscillations, Norwell, Massachusetts 02061 USA: Kluwer Academic Publishers, 2000.

[41] Lucas Lugnani Fernandes, Daniel Dotta, Joao M F Ferreira und I.C. Decker, „Frequency Response Estimation Following Large Disturbances using Synchrophasors," in *IEEE PES GM 2018*, Portland, March 2018.

[42] A. Ahmed, O. Z. Amer und Y. A. Mobarak , „POWER SYSTEM DAMPING ENHANCEMENT VIA COORDINATED DESIGN OF PSS & TCSC," *Engineering Sciences, Assiut University,* Bde. %1 von %2Vol. 39, No 1, pp. 113-122, January 2011 .

[43] Chandrasekar Samudi und Kusumakumari.P, „Power System Stabilizer Design Using Local and Global signals".

[44] C. A. F. D. Taouba Jouini, „Grid-Friendly Matching of Synchronous Machines by Tapping into the DC Storage," Nr. ETH funds and the SNF Assistant Professor Energy Grant #160573.

[45] „Ren21, GLOBAL STATUS REPORT," 2012. [Online]. Available: https://www.ren21.net/reports/ren21-reports/. [Zugriff am September 2020].

Eidesstattliche Erklärung

Hiermit erkläre ich, dass die vorliegende Arbeit gemäß dem Code of Conduct, insbesondere ohne unzulässige Hilfe Dritter und ohne Benutzung anderer als der angegebenen Hilfsmittel, angefertigt wurde. Die aus anderen Quellen direkt oder indirektübernommenen Daten und Konzepte sind unter Angabe der Quellen gekennzeichnet. Die Arbeit wurde bisher weder im In- noch Ausland in gleicher oder ähnlicher Form in anderen Prüfungsverfahren vorgelegt.

Oktober, 2020

Alireza Kerdegarbakhsh